Early acquisition of S-specific Tfh clonotypes after SARS-CoV-2 vaccination is associated with the longevity of anti-S antibodies

Xiuyuan Lu[1, ¶], Hiroki Hayashi[2, ¶], Eri Ishikawa[1, 3, ¶], Yukiko Takeuchi[1], Julian Vincent Tabora Dychiao[1], Hironori Nakagami[2, *] and Sho Yamasaki[1, 3, 4, *]

[1] Laboratory of Molecular Immunology, Immunology Frontier Research Center, Osaka University, Suita, Osaka, Japan

[2] Department of Health Development and Medicine, Osaka University Graduate School of Medicine, Suita, Osaka, Japan

[3] Department of Molecular Immunology, Research Institute for Microbial Diseases, Osaka University, Suita, Osaka, Japan

[4] Center for Infectious Disease Education and Research (CiDER), Osaka University, Suita, Osaka, Japan

¶These three authors contributed equally to this work.

[*] Co-corresponding authors

Sho Yamasaki: yamasaki@biken.osaka-u.ac.jp

Hironori Nakagami: nakagami@gts.med.osaka-u.ac.jp

Abstract

SARS-CoV-2 vaccines have been used worldwide to combat COVID-19 pandemic. To elucidate the factors that determine the longevity of spike (S)-specific antibodies, we traced the characteristics of S-specific T cell clonotypes together with their epitopes and anti-S antibody titers before and after BNT162b2 vaccination over time. T cell receptor (TCR) αβ sequences and mRNA expression of the S-responded T cells were investigated using single-cell TCR- and RNA-sequencing. Highly expanded 199 TCR clonotypes upon stimulation with S peptide pools were reconstituted into a reporter T cell line for the determination of epitopes and restricting HLAs. Among them, we could determine 78 S epitopes, most of which were conserved in variants of concern (VOCs). In donors exhibiting sustained anti-S antibody titers (designated as "sustainers"), S-reactive T cell clonotypes detected immediately after 2nd vaccination polarized to follicular helper T (Tfh)-like cells, which was less obvious in "decliners". Even before vaccination, S-reactive $CD4^+$ T cell clonotypes did exist, most of which cross-reacted with environmental or symbiotic bacteria. However, these clonotypes contracted after vaccination. Conversely, S-reactive clonotypes dominated after vaccination were undetectable in pre-vaccinated T cell pool, suggesting that highly-responding S-reactive T cells were established by vaccination from rare clonotypes. These results suggest that *de novo* acquisition of memory Tfh-like cells upon vaccination contributes to the longevity of anti-S antibody titers.

42 **Introduction**

43 The pandemic COVID-19, caused by the severe acute respiratory syndrome
44 coronavirus 2 (SARS-CoV-2), has expanded worldwide [1]. Many types of vaccines have been
45 developed or in basic and clinical phases to combat infection and deterioration of COVID-19
46 [2,3]. Among them, messenger ribonucleic acid (mRNA) vaccines, BNT162b2/Comirnaty and
47 mRNA-1273/Spikevax, have been approved with over 90% efficacy at 2 months post-2nd dose
48 vaccination [4,5], and widely used. Pathogen-specific antibodies are one of the most efficient
49 components to prevent infection. Yet, mRNA vaccine-induced serum antibody titer is known
50 to be waning over 6 months [6,7]. Accordingly, the effectiveness of the vaccines decreases
51 over time, and thus multiple doses and repeated boosters are necessary [8].

52 The production and sustainability of spike (S)-specific antibody could be related to
53 multiple factors, especially in the case of humans [7,9]. Among them, the characteristics of
54 SARS-CoV-2-specific T cells is critically involved in the affinity and longevity of the
55 antibodies [10–12]. Elucidation of the key factors of T cell responses that contribute to the
56 durable immune responses induced by vaccination would provide valuable information for the
57 vaccine development in the future. However, the relationship between antibody sustainability
58 and the types of antigen-specific T cells has not been investigated in a clonotype resolution.

59 Recent studies reported that S-reactive T cells pre-existed before exposure to SARS-
60 CoV-2 [13–17]. Common cold human coronaviruses (HCoVs) including strains 229E, NL63,
61 OC43, and HKU1 are considered major cross-reactive antigens that primed these pre-existing
62 T cells [15,18–20], while bacterial cross-reactive antigens were also reported [21,22]. However,
63 the functional relevance of cross-reactive T cells during infection or vaccination is still in
64 debate.

65 In this study, both humoral and cellular immune responses were evaluated at 3, 6 and
66 24 weeks after BNT162b2/Comirnaty vaccination. S-specific T cells before and after

67 vaccination were analyzed on clonotype level using single cell-based T cell receptor (TCR)
68 and RNA sequencing to determine their characteristics and epitopes in antibody sustainers and
69 decliners. These analyses suggest the importance of early acquisition of S-specific Tfh cells in
70 the longevity of antibodies.

71 **Results**

72 **SARS-CoV-2 mRNA vaccine elicits transient humoral immunity**

73 Blood samples were collected from a total of 43 individuals (Table 1) who had no
74 SARS-CoV-2 infection history when they received two doses of SARS-CoV-2 mRNA vaccine
75 BNT162b2. Samples were taken before and after the vaccination (Fig. 1A). Consistent with
76 the previous report [4], most participants exhibited more severe side effects after 2nd dose of
77 vaccination than 1st dose locally (Table 2) and systemically (Table 3). At 3 weeks, anti-S IgG
78 antibody titer increased in most participants. At 6 weeks, anti-S antibody titer was at its peak.
79 S antibody titer gradually decreased over 24 weeks (Fig. 1B). The antibody titer was reduced
80 by 56.8% on average. Donors of different genders or age groups showed no significant
81 difference in anti-S antibody titer (Fig. S1). The neutralization activity of the post-vaccinated
82 sera showed similar tendency with the anti-S antibody titer during the study period (Fig. 1C).
83 The above results indicate that the mRNA vaccine effectively activated humoral immune
84 responses in healthy individuals, but decreased by 24 weeks over time as reported [6,7].

85

86 **Antibody sustainers had highly expanded S-reactive Tfh clonotypes**

87 To address the role of T cells in maintaining the antibody titer, we analyzed the S-
88 responsive T cells in the post-vaccination samples from 8 donors, among whom 4 donors
89 showed relatively sustained anti-S antibody titer during 6 weeks to 24 weeks (reduction < 30%)
90 (sustainers, donors #8, #25, #27 and #28), while the other 4 donors showed largely declined
91 anti-S antibody titer (reduction > 80%) (decliners, donors #4, #13, #15 and #17) (Fig. 2A and
92 Fig. S2A). The possibility of SARS-CoV-2 infection of sustainers was ruled out by analyzing
93 anti-nucleocapsid protein (N) antibody titer in the sera samples at 24 weeks (Fig. S2B).
94 Antibody sustainability did not correlate with bulk T cell responses to S protein, such as IFNγ
95 production (Fig. S2C).

96 To enrich the S-reactive T cells, we labeled the peripheral blood mononuclear cells
97 (PBMCs) with a cell proliferation tracer and stimulated the PBMCs with an S peptide pool for
98 10 days. Proliferated T cells were sorted and analyzed by single-cell TCR- and RNA-
99 sequencing (scTCR/RNA-seq). Clustering analysis was done with pooled samples of 3 time
100 points from 8 donors, and various T cell subtypes were identified (Fig. 2B). We found that,
101 overall, the S-reactive T cells did not skew to any particular T cell subset (Fig. 2B). However,
102 by grouping the cells from decliners and sustainers separately, we found difference in the
103 frequency of the cells within the circled population (Fig. 2C), and overall, the sustainer
104 individuals had more cells in this region (Fig. S3). These cells showed high Tfh signature scores
105 and expressed characteristic genes of Tfh cells (Fig. 2D). This tendency became more
106 pronounced when we selected highly expanded (top 16) clonotypes in each donor (Fig. 2E). In
107 sustainers, S-specific Tfh clusters appeared from 6 weeks (Fig. 2F), suggesting that vaccine-
108 induced Tfh-like cells that have potency of deriving to Tfh cells were established immediately
109 after 2nd vaccination.
110
111 **Identification of dominant S epitopes recognized by vaccine-induced T cell clonotypes**
112 To elucidate the epitopes of the highly expanded clonotypes, we reconstituted their
113 TCRs into a T cell hybridoma lacking endogenous TCRs and having an NFAT-GFP reporter
114 gene. These cell lines were stimulated with S peptides using transformed autologous B cells as
115 antigen-presenting cells (APCs). The epitopes of 53 out of 128 reconstituted clonotypes were
116 successfully determined (Fig. 3, Table 4, Figs. S4A–S4D). Epitopes of expanded Tfh cells were
117 not limited in any particular region of S protein (Fig. 3). About 72% of these epitopes conserved
118 in Delta and Omicron variants (Tables 4 and 5). Within the rest of 28% of epitopes which were
119 mutated in variants of concerns (VOCs), although some mutated epitopes located in the
120 receptor-binding domain (RBD) of VOCs lost antigenicity, recognition of most epitopes

121 outside the RBD region was maintained or rather increased in the variants (Table 5 and Figs.
122 S4E and S4F). These results suggest that the majority of S-reactive clonotypes after vaccination
123 can respond to antibody-escaping VOCs.
124
125 **Identification of S epitopes and cross-reactive antigens of pre-existing T cell clonotypes**
126 Before the pandemic, T cells cross-reacting to S antigen were present in the peripheral
127 blood [13–17]. To characterize these pre-existing S-reactive cells, we analyzed the PBMCs
128 collected from donors who consented to blood sample donation before vaccination (#4, #8, #13,
129 #15, and #17). PBMCs were stimulated with the S peptide pool for 10 days, and proliferated T
130 cells were sorted and analyzed by scTCR/RNA-seq. Similar to vaccine-induced S-reactive T
131 cells (Fig. 2B), characteristics of pre-existing S-reactive T cells were diverse (Fig. 4A). To
132 track the dynamics of cross-reactive clones after vaccination, we combined the single-cell
133 sequencing data of pre- and post-vaccinated PBMCs and analyzed the clonotypes that have
134 more than 50 cells in total (Fig. 4B). We did find some cross-reactive clonotypes that were
135 further expanded by vaccination, and most of these clonotypes had cytotoxic features, being
136 $CD8^+$ effector memory T cells (Tem) or minor $CD4^+$ cytotoxic T cells (CTLs). In contrast,
137 most of the cross-reactive $CD4^+$ T cells became minor clonotypes after vaccination.
138 We also explored the epitopes of the top 16 expanded clonotypes in each pre-vaccinated
139 donor by reconstituting the TCRs into reporter cell lines. We identified 18 epitopes from S
140 protein (Fig. 5 and Table 6) and determined some possible cross-reactive antigens. Most of
141 these cross-reactive antigens originated from environmental or symbiotic microbes (Table 6).
142 Furthermore, majority of the reactive T clonotypes showed regulatory T cell (Treg) signatures
143 (Fig. 5). Six of these 80 analyzed clonotypes could also be frequently detected in the public
144 TCR database Adaptive [23,24]. Notably, most of these clonotypes, except for one case,
145 showed comparable frequencies between pre-pandemic healthy donors and COVID-19

146 convalescent patients (Fig. 6), suggesting that these clonotypes did not expand upon SARS-
147 CoV-2 infection, despite they were present before the pandemic. Thus, it is unlikely that these
148 cross-reactive T clonotypes contribute to the establishment of S-reactive T cell pools during
149 either vaccination or infection.

150 **Discussion**

151 Previous studies showed that Tfh function and germinal center development were
152 impaired in deceased COVID-19 patients [25] and Tfh cell number correlated with neutralizing
153 antibody [26–28]. Consistent with the above studies, we found that the donors having sustained
154 antibody titers between 6 to 24 weeks post-vaccination had more S antigen-responsive Tfh-
155 like clonotypes maintained in the periphery as a memory pool. As circulating Tfh clonotypes
156 can reflect the population of germinal center Tfh cells [29], it is possible that these maintained
157 S-responsive Tfh cells contribute to the prolonged production of anti-S antibodies. These
158 results imply that Tfh polarization of S-reactive T cells in the blood after 2nd vaccination can
159 be a marker for the longevity of serum anti-S antibodies. Although monitoring of S-specific
160 Tfh cells in germinal center is ideal [30], it is currently difficult for outpatients in clinics.

161 Since the antigen used for BNT162b2 is a full-length S protein from the Wuhan-Hu-1
162 strain, it is important to estimate whether vaccine-induced Wuhan S-reactive T cells recognize
163 neutralizing antibody-evading VOCs, such as Omicron variants. To investigate the dominant
164 T cell epitopes of vaccine-developed T cells, we utilized a proliferation-based sorting strategy
165 to enrich the S-responsive T cells. The limitation of this strategy is that a 10-day stimulation
166 would change the transcriptional profile and repertoire of T cells. However, This strategy
167 allowed us to select the T cell clonotypes that vigorously responded to the S antigen stimulation,
168 while weakly responsive cells and anergic cells will be less considered, which is exactly in line
169 with our purpose. Consistent with previous reports [31–33], most of the epitopes determined
170 in the current study were conserved in Delta and Omicron (BA.1, BA.2 and BA.4/5) strains,
171 suggesting that vaccine-induced T cells are able to recognize the mutated S proteins from these
172 variants, despite B epitopes being largely mutated in these VOCs [31,32].

173 SARS-CoV-2-recognizing T cells existed prior to exposure to the S antigens [13–17],
174 which is consistent with our observation with PBMCs from donors who were uninfected and

175 pre-vaccinated. Among these pre-existing S-reactive clonotypes, $CD8^+$ cytotoxic T clonotypes
176 were expanded by the vaccination, whereas most of $CD4^+$ T clonotypes became less dominant
177 after vaccination (Fig. 4B). Currently, the reason for the opposite tendency is unclear. In the
178 present study, we showed that pre-existing T clonotypes cross-reacting to S protein are unlikely
179 to contribute to vaccine-driven T cell immunity. This could be due to the fact that cross-reactive
180 T cells had relatively low avidity to S protein [34]. Alternatively, but not mutually exclusively,
181 considering that most of these cross-reactive T clonotypes have Treg signature (Fig. 5), they
182 could be developed to tolerate symbiotic or environmental antigens, and might be ineffective
183 to the defense against SARS-CoV-2 and thus replaced by the other effective T clonotypes
184 induced by vaccination. One exceptional pre-existing clonotype was #15-Pre_2, as they
185 vigorously expanded in COVID-19 patients (Fig. 6). This clonotype was clustered within a
186 $CD4^+$ Tem population and cross-reactive to environmental bacteria, *Myxococcales bacterium*
187 (Table 6). Thus, in some particular settings, clonotypes primed by common bacterial antigens
188 might potentially contribute during infection.

189 Common cold human coronavirus (HCoV)-derived S proteins are reported as potential
190 cross-reactive antigens for pre-existing SARS-CoV-2 S-reactive T cells [15,18–20]. However,
191 the highly responding SARS-CoV-2 S-reactive clonotypes in pre-vaccinated donors did not
192 react with HCoV S proteins in the present study (Fig. S5), which might be partly due to the
193 difference of cohorts or ethnicities. Instead, most of those T cells cross-reacted with
194 environmental or symbiotic bacteria. These observations suggest that these cross-reactive T
195 cells might have been developed to establish tolerance against less harmful microbes, and thus
196 unlikely to efficiently contribute to the protective viral immunity. Vaccination may induce
197 opposite tendencies on T cell clonotypes that recognize the same antigen [35], which is hardly
198 detected by the bulk T cell analyses. The current study highlights the necessity of dynamic

199 tracing of T cell responses in an epitope-specific clonotype resolution for the evaluation of
200 vaccine-induced immunity.

201 The limitation of this study is the number of individuals we analyzed. However,
202 chronological and clonological analysis of antigen-specific T cells in characteristic groups
203 followed by epitope determination has not been performed before. This study suggests that
204 mRNA vaccine is potent enough to prime rare T cell clonotypes that become dominant
205 afterwards. Furthermore, we propose that the types of $CD4^+$ T clonotypes developed shortly
206 after two doses of vaccination could be an indication of the longevity of antibodies in the
207 following months. Tfh-inducing adjuvants or Tfh-skewing epitope would be a promising
208 "directional" booster in the post-vaccine era when most people worldwide were exposed with
209 the same antigen in multiple doses within a short period. Furthermore, in addition to SARS-
210 CoV-2, this strategy can also be applicable for the prevention of other infectious diseases of
211 which neutralizing antibody titers are effective for protection.

212 **Materials and Methods**

213 *Ethics statement and sample collection*

214 This project was approved by Osaka University Institutional Review Board (IRB) (reference
215 No. 21487). 43 volunteers were enrolled in this project. Informed consent was obtained from
216 all participants before the first blood sampling. Samples (serum, whole blood, and PBMCs)
217 were collected four times at 0–7 days before 1st dose vaccination as pre-vaccination, at 14–21
218 days after 1st dose vaccination as 3 weeks sample, at 35–49 days after 1st dose vaccination as
219 6 weeks sample, and at 154–182 days after 1st dose of vaccination as 24 weeks sample. At the
220 same time of blood sampling, adverse event information was also collected from all
221 participants. PBMCs were isolated using BD vacutainer® CPT™ cell separation tube (Beckton
222 Dickinson), according to manufacturers' instructions. Isolated PBMCs were stored in the vapor
223 phase of liquid nitrogen until use.

224

225 *Antibody titer determination by enzyme-linked immunosorbent assay (ELISA)*

226 Serum antibody titer was measured using ELISA. Briefly, recombinant ancestral S protein
227 (S1+S2, Cell Signaling Technology; 1 μg/ml) or recombinant nucleocapsid protein
228 (Acrobiosystems; 1 μg/ml) was coated on 96-well plate at 4 °C overnight. On the second day,
229 wells were blocked with blocking buffer (PBS-T (0.05% tween®20) containing 5% skim milk)
230 for 2 h at room temperature. The sera were diluted from 10 to 31,250 folds in blocking buffer
231 and incubated overnight at 4 °C. The next day, wells were washed and incubated with
232 horseradish peroxidase (HRP)-conjugated antibodies (GE Healthcare) for 3 h at room
233 temperature. After being washed with PBS-T, wells were incubated with the peroxidase
234 chromogenic substrate 3,3'-5,5'-tetramethyl benzidine (Sigma-Aldrich) for 30 min at room
235 temperature, then the reaction was stopped by 0.5 N sulfuric acid (Sigma Aldrich). The
236 absorbance of wells was immediately measured at 450 nm with a microplate reader (Bio-Rad).

237 The value of the half-maximal antibody titer of each sample was calculated from the highest
238 absorbance in the dilution range by using Prism 8 software. The calculated antibody titer was
239 converted to BAU/ml by using WHO International Standard 20/136 (NIBSC) for ancestral S-
240 specific antibody titer.
241
242 *Whole blood interferon-gamma release immune assay (IGRA) for SARS-CoV-2 specific T cell*
243 *responses using QuantiFERON*
244 SARS-CoV-2 specific T cell immune responses were evaluated by QuantiFERON SARS-
245 CoV-2 (Qiagen) [36], according to manufacturer's instructions, in which $CD4^+$ T cells were
246 activated by epitopes coated on Ag1 tube, and $CD4^+$ and $CD8^+$ T cells were activated by
247 epitopes coated on Ag2 tube. Briefly, 1 ml of whole blood sample with heparin is added into
248 each of Nil (negative control), Mito (positive control), Ag1, and Ag2 tubes, and incubated at
249 37 °C for 22–24 h. Tubes were then centrifuged at 3,000 × g for 15 min for collecting plasma
250 samples. IFNγ derived from activated T cells was measured with enzyme-linked
251 immunosorbent assay (ELISA) (Qiangen) according to the manufacturer's instructions. IFNγ
252 concentration (IU/ml) was calculated with background (Nil tube) subtracted from values of
253 Ag1 or Ag2 tubes.
254
255 *Pseudo-typed virus neutralization assay*
256 The neutralizing activity of serum antibodies was analyzed with pseudo-typed VSVs as
257 previously described [37]. Briefly, Vero E6 cells stably expressing TMPRSS2 were seeded on
258 96-well plates and incubated at 37 °C for 24 h. Pseudoviruses were incubated with a series of
259 dilutions of inactivated serum for 1 h at 37 °C, then added to Vero E6 cells. At 24 h after
260 infection, cells were lysed with cell culture lysis reagent (Promega), and luciferase activity was
261 measured by Centro XS^3 LB 960 (Berthold).

262

263 *In vitro stimulation of PBMCs*

264 Cryopreserved PBMCs were thawed and washed with warm RPMI 1640 medium (Sigma)
265 supplemented with 5% human AB serum (GeminiBio), Penicillin (Sigma), streptomycin (MP
266 Biomedicals), and 2-mercaptoethanol (Nacalai Tesque). PBMCs were labeled with Cell
267 Proliferation Kit (CellTrace™ Violet, ThermoFisher) following the manufacturer's protocol
268 and were stimulated in the same medium with S peptide pool (1 μg/ml per peptide, JPT) for 10
269 days, with human recombinant IL-2 (1 ng/ml, Peprotech), IL-7 (5 ng/ml, BioLegend) and IL-
270 15 (5 ng/ml, Peprotech) supplemented on day 2, day 5 and day 8 of the culture. On day 10 cells
271 were washed and stained with anti-human CD3 and TotalSeq-C Hashtags antibodies.
272 Proliferated T cells ($CD3^{+}CTV^{low}$) were sorted by cell sorter SH800S (SONY) and used for
273 single-cell TCR and RNA sequencing analyses.

274

275 *Single cell-based transcriptome and TCR repertoire analysis*

276 Single cell library was prepared using the reagents from 10x Genomics following the
277 manufacturer's instructions. After reverse transcription, cDNA was amplified for 14 cycles,
278 and up to 50 ng of cDNA was used for construction of gene expression and TCR libraries.
279 Libraries were sequenced in paired-end mode, and the raw reads were processed by Cell Ranger
280 6.0.0 (10x Genomics). Distribution of the mitochondrial gene percentage, n_counts and
281 n_genes were fitted with a one-variable, two-component mixed Gaussian model using the
282 Python package scikit-learn [38] and divided into two distributions corresponding to high and
283 low levels, respectively. The cutting threshold values were the middle value of the means of
284 the two fitted Gaussian distributions. A package call Scrublet was also applied [39], and the
285 events whose main hashtag reads are less than 95% of the total hashtag reads were gated out
286 before the UMAP plots were exported using BBrowser [40]. Tfh signature score was generated

287 using canonical Tfh marker genes (*IL21*, *ICOS*, *CD200, PDCD1*, *POU2AF1*, *BTLA*, *CXCR5,*
288 and *CXCL13*). Other cell populations were annotated using the following markers: Treg,
289 $CD4^{+}FOXP3^{+}$; CD4T, $CD3E^{+}CD4^{+}$; CD8T, $CD3E^{+}CD8A^{+}$; central memory (cm) cells,
290 *SELL*(CD62L)^{hi} cells although sometimes *CCR7* expression is vague; effector memory (em)
291 cells, $SELL^{low/-}CCR7^{-}$ and *IFNG*-expressing cells containing populations; naïve cells,
292 $CCR7^{+}TCF7^{+}$; cycling cells, $MKI67^{hi}$; γδT, $TRDC^{+}$; B cells, $CD19^{+}$; Monocyte, $CD14^{+}$; MAIT,
293 $CD3E^{+}KLRB1^{+}IL18R1^{+}$; Tfr, $FOXP3^{+}NRN1^{+}$ in cells with high Tfh score; CD4-CTL, $GZMB^{+}$
294 in CD4T cells [14,41–43].
295
296 *Reporter cell establishment and stimulation*
297 TCRα and β chain cDNA sequences were introduced into a mouse T cell hybridoma lacking
298 TCR and having a nuclear factor of activated T-cells (NFAT)-green fluorescent protein (GFP)
299 reporter gene [44] using retroviral vectors. TCR-reconstituted cells were co-cultured with 1
300 μg/ml of peptides in the presence of antigen-presenting cells (APCs). After 20 h, cell activation
301 was assessed by GFP and CD69 expression.
302
303 *Antigen-presenting cells*
304 Transformed B cells and HLA-transfected HEK293T cells used as APCs were generated as
305 described [21]. For transformed B cells, 3×10^{5} PBMCs were incubated with the recombinant
306 Epstein-Barr virus (EBV) suspension [45] for 1 h at 37°C with mild shaking every 15 min. The
307 infected cells were cultured in RPMI 1640 medium supplemented with 20% fetal bovine serum
308 (FBS, CAPRICORN SCIENTIFIC GmbH) containing cyclosporine A (CsA, 0.1 μg/ml,
309 Cayman Chemical). Immortalized B lymphoblastoid cell lines were obtained after 3 weeks of
310 culture and used as APCs. For HLA-transfected HEK293T cells, plasmids encoding HLA class
311 I/II alleles [46] were transfected in HEK293T cells with PEI MAX (Polysciences).

312

313 *Determination of epitopes and restricting HLA*

314 15-mer peptides with 11 amino acids overlap that cover the full length of S protein of SARS-
315 CoV-2 were synthesized (GenScript). Peptides were dissolved in DMSO at 12 mg/ml and 12-
316 15 peptides were mixed to create 26 different semi-pools. TCR-reconstituted reporter cells
317 were stimulated with 1 μg/ml of S peptide pool (1 μg/ml per peptide, JPT), then 36-peptide
318 pools that consist of 3 semi-pools each, then semi-pools, and then 12 individual peptides in the
319 presence of autologous B cells to identify epitope peptides. To determine the restricting HLA,
320 HLAs were narrowed down by co-culturing reporter cells with autologous and various
321 heterologous B cells in the presence of 1 μg/ml of the epitope peptide. HLAs shared by
322 activatable B cells were transduced in HEK239T cells and used for further co-culture to
323 identify the restricting HLA.

324

325 *Statistics*

326 All values with error bars are presented as the mean ± SEM. One-way ANOVA followed by
327 Turkey's post hoc multiple comparison test was used to assess significant differences in each
328 experiment using Prism 8 software (GraphPad Software). Differences were considered to be
329 significant when *P* value was less than 0.05. *P* values in Fig. 6 were calculated with t-test using
330 the "stat_compare_means" function in R.

331 **Data availability**

332 Single cell-based transcriptome data have been deposited in Gene Expression Omnibus (GEO)
333 datasets (accession number GSE246535). Other data needed to support the conclusion of this
334 manuscript are included in the main text and Supplemental information.

335 **Acknowledgements**

336 We thank S. Iwai, Y. Sakai, C. Günther, J. Sun, and Y. Yanagida for experimental support, D.
337 Motooka, D. Okuzaki, and YC. Liu for bioinformatic data analysis and C. Schutt and Y.
338 Yamagishi for discussion. This research was supported by Japan Agency for Medical Research
339 and Development (JP223fa627002, JP223fa727001, JP23ym0126049 (SY), JP21ym0126049
340 (HN)) and Japan Society for the Promotion of Science Grants-in-Aid for Scientific Research
341 (JP20H00505, JP22H05182, JP22H05183 (SY)). The Department of Health Development and
342 Medicine is an endowed department supported by AnGes, Daicel, and FunPep.

References

1. Hu B, Guo H, Zhou P, Shi ZL. Characteristics of SARS-CoV-2 and COVID-19. Nature Reviews Microbiology 2020 19:3. 2021;19: 141–154. doi:10.1038/s41579-020-00459-7
2. Krammer F. SARS-CoV-2 vaccines in development. Nature. 2020;586: 516–527. doi:10.1038/s41586-020-2798-3
3. Creech CB, Walker SC, Samuels RJ. SARS-CoV-2 Vaccines. JAMA. 2021;325: 1318–1320. doi:10.1001/JAMA.2021.3199
4. Polack FP, Thomas SJ, Kitchin N, Absalon J, Gurtman A, Lockhart S, et al. Safety and Efficacy of the BNT162b2 mRNA Covid-19 Vaccine. New England Journal of Medicine. 2020;383: 2603–2615. doi:10.1056/NEJMOA2034577
5. Baden LR, el Sahly HM, Essink B, Kotloff K, Frey S, Novak R, et al. Efficacy and Safety of the mRNA-1273 SARS-CoV-2 Vaccine. New England Journal of Medicine. 2021;384: 403–416. doi:10.1056/nejmoa2035389
6. Pegu A, O'Connell SE, Schmidt SD, O'Dell S, Talana CA, Lai L, et al. Durability of mRNA-1273 vaccine-induced antibodies against SARS-CoV-2 variants. Science (1979). 2021;373: 1372–1377. doi:10.1126/SCIENCE.ABJ4176
7. Levin EG, Lustig Y, Cohen C, Fluss R, Indenbaum V, Amit S, et al. Waning Immune Humoral Response to BNT162b2 Covid-19 Vaccine over 6 Months. New England Journal of Medicine. 2021;385: e84. doi:10.1056/NEJMOA2114583
8. Andrews N, Stowe J, Kirsebom F, Toffa S, Rickeard T, Gallagher E, et al. Covid-19 Vaccine Effectiveness against the Omicron (B.1.1.529) Variant. New England Journal of Medicine. 2022;386: 1532–1546. doi:10.1056/NEJMoa2119451
9. Collier DA, de Marco A, Ferreira IATM, Meng B, Datir RP, Walls AC, et al. Sensitivity of SARS-CoV-2 B.1.1.7 to mRNA vaccine-elicited antibodies. Gabriela Barcenas-Morales. 2021;593: 136. doi:10.1038/s41586-021-03412-7
10. Nelson RW, Chen Y, Venezia OL, Majerus RM, Shin DS, Carrington MN, et al. SARS-CoV-2 epitope–specific CD4+ memory T cell responses across COVID-19 disease severity and antibody durability. Sci Immunol. 2022;7: 9464. doi:10.1126/SCIIMMUNOL.ABL9464
11. Terahara K, Sato T, Adachi Y, Tonouchi K, Onodera T, Moriyama S, et al. SARS-CoV-2-specific CD4+ T cell longevity correlates with Th17-like phenotype. iScience. 2022;25: 104959. doi:10.1016/J.ISCI.2022.104959
12. Crotty S. T Follicular Helper Cell Biology: A Decade of Discovery and Diseases. Immunity. 2019;50: 1132–1148. doi:10.1016/j.immuni.2019.04.011
13. Grifoni A, Weiskopf D, Ramirez SI, Mateus J, Dan JM, Moderbacher CR, et al. Targets of T Cell Responses to SARS-CoV-2 Coronavirus in Humans with COVID-19 Disease and Unexposed Individuals. Cell. 2020;181: 1489-1501.e15. doi:10.1016/j.cell.2020.05.015
14. Meckiff BJ, Ramírez-Suástegui C, Fajardo V, Chee SJ, Kusnadi A, Simon H, et al. Imbalance of Regulatory and Cytotoxic SARS-CoV-2-Reactive CD4+ T Cells in COVID-19. Cell. 2020; 1–14. doi:10.1016/j.cell.2020.10.001
15. Mateus J, Grifoni A, Tarke A, Sidney J, Ramirez SI, Dan JM, et al. Selective and cross-reactive SARS-CoV-2 T cell epitopes in unexposed humans. Science (1979). 2020;370: 89–94. doi:10.1126/science.abd3871
16. Sekine T, Perez-Potti A, Rivera-Ballesteros O, Strålin K, Gorin JB, Olsson A, et al. Robust T Cell Immunity in Convalescent Individuals with Asymptomatic or Mild COVID-19. Cell. 2020;183: 158-168.e14. doi:10.1016/j.cell.2020.08.017

392 17. le Bert N, Tan AT, Kunasegaran K, Tham CYL, Hafezi M, Chia A, et al. SARS-CoV-
393 2-specific T cell immunity in cases of COVID-19 and SARS, and uninfected controls.
394 Nature. 2020;584: 457–462. doi:10.1038/s41586-020-2550-z
395 18. Loyal L, Braun J, Henze L, Kruse B, Dingeldey M, Reimer U, et al. Cross-reactive
396 CD4+ T cells enhance SARS-CoV-2 immune responses upon infection and
397 vaccination. Science (1979). 2021;374. doi:10.1126/science.abh1823
398 19. Low JS, Vaqueirinho D, Mele F, Foglierini M, Jerak J, Perotti M, et al. Clonal analysis
399 of immunodominance and crossreactivity of the CD4 T cell response to SARS-CoV-2.
400 Science (1979). 2021;372: 1336–1341. doi:10.1126/science.abg8985
401 20. Becerra-Artiles A, Calvo-Calle JM, Co MD, Nanaware PP, Cruz J, Weaver GC, et al.
402 Broadly recognized, cross-reactive SARS-CoV-2 CD4 T cell epitopes are highly
403 conserved across human coronaviruses and presented by common HLA alleles. Cell
404 Rep. 2022;39: 110952. doi:10.1016/J.CELREP.2022.110952
405 21. Lu X, Hosono Y, Nagae M, Ishizuka S, Ishikawa E, Motooka D, et al. Identification of
406 conserved SARS-CoV-2 spike epitopes that expand public cTfh clonotypes in mild
407 COVID-19 patients. Journal of Experimental Medicine. 2021;218.
408 doi:10.1084/jem.20211327
409 22. Bartolo L, Afroz S, Pan Y-G, Xu R, Williams L, Lin C-F, et al. SARS-CoV-2-specific
410 T cells in unexposed adults display broad trafficking potential and cross-react with
411 commensal antigens. Sci Immunol. 2022;7. doi:10.1126/sciimmunol.abn3127
412 23. Emerson RO, DeWitt WS, Vignali M, Gravley J, Hu JK, Osborne EJ, et al.
413 Immunosequencing identifies signatures of cytomegalovirus exposure history and
414 HLA-mediated effects on the T cell repertoire. Nat Genet. 2017;49: 659–665.
415 doi:10.1038/ng.3822
416 24. Nolan S, Vignali M, Klinger M, Dines JN, Kaplan IM, Craft T, et al. A large-scale
417 database of T-cell receptor beta (TCR β) sequences and binding associations from
418 natural and synthetic exposure to SARS-CoV-2. Res Sq. 2020; 10.21203/RS.3.RS-
419 51964/V1. doi:10.21203/RS.3.RS-51964/V1
420 25. Kaneko N, Kuo HH, Boucau J, Farmer JR, Allard-Chamard H, Mahajan VS, et al.
421 Loss of Bcl-6-Expressing T Follicular Helper Cells and Germinal Centers in COVID-
422 19. Cell. 2020;183: 143-157.e13. doi:10.1016/j.cell.2020.08.025
423 26. Gong F, Dai Y, Zheng T, Cheng L, Zhao D, Wang H, et al. Peripheral CD4+ T cell
424 subsets and antibody response in COVID-19 convalescent individuals. Journal of
425 Clinical Investigation. 2020;130: 6588–6599. doi:10.1172/JCI141054
426 27. Juno JA, Tan HX, Lee WS, Reynaldi A, Kelly HG, Wragg K, et al. Humoral and
427 circulating follicular helper T cell responses in recovered patients with COVID-19.
428 Nat Med. 2020;26: 1428–1434. doi:10.1038/s41591-020-0995-0
429 28. Zhang J, Wu Q, Liu Z, Wang Q, Wu J, Hu Y, et al. Spike-specific circulating T
430 follicular helper cell and cross-neutralizing antibody responses in COVID-19-
431 convalescent individuals. Nature Microbiology 2020 6:1. 2021;6: 51–58.
432 doi:10.1038/s41564-020-00824-5
433 29. Brenna E, Davydov AN, Ladell K, McLaren JE, Bonaiuti P, Metsger M, et al. CD4 +
434 T Follicular Helper Cells in Human Tonsils and Blood Are Clonally Convergent but
435 Divergent from Non-Tfh CD4 + Cells. Cell Rep. 2020;30: 137-152.e5.
436 doi:10.1016/J.CELREP.2019.12.016
437 30. Mudd PA, Minervina AA, Pogorelyy M v., Turner JS, Kim W, Kalaidina E, et al.
438 SARS-CoV-2 mRNA vaccination elicits a robust and persistent T follicular helper cell
439 response in humans. Cell. 2022;185: 603-613.e15. doi:10.1016/J.CELL.2021.12.026
440 31. Tarke A, Coelho CH, Zhang Z, Dan JM, Yu ED, Methot N, et al. SARS-CoV-2
441 vaccination induces immunological T cell memory able to cross-recognize variants

442 from Alpha to Omicron. Cell. 2022;185: 847-859.e11.
443 doi:10.1016/J.CELL.2022.01.015
444 32. GeurtsvanKessel CH, Geers D, Schmitz KS, Mykytyn AZ, Lamers MM, Bogers S, et
445 al. Divergent SARS-CoV-2 Omicron–reactive T and B cell responses in COVID-19
446 vaccine recipients. Sci Immunol. 2022;7: eabo2202. doi:10.1126/sciimmunol.abo2202
447 33. Keeton R, Tincho MB, Ngomti A, Baguma R, Benede N, Suzuki A, et al. T cell
448 responses to SARS-CoV-2 spike cross-recognize Omicron. Nature. 2022;603: 488–
449 492. doi:10.1038/s41586-022-04460-3
450 34. Bacher P, Rosati E, Esser D, Martini GR, Saggau C, Schiminsky E, et al. Low-Avidity
451 CD4+ T Cell Responses to SARS-CoV-2 in Unexposed Individuals and Humans with
452 Severe COVID-19. Immunity. 2020;53: 1258-1271.e5.
453 doi:10.1016/j.immuni.2020.11.016
454 35. Aoki H, Kitabatake M, Abe H, Shichino S, Hara A, Ouji-Sageshima N, et al. T cell
455 responses induced by SARS-CoV-2 mRNA vaccination are associated with clonal
456 replacement. bioRxiv. 2022; 2022.08.27.504955. doi:10.1101/2022.08.27.504955
457 36. Jaganathan S, Stieber F, Rao SN, Nikolayevskyy V, Manissero D, Allen N, et al.
458 Preliminary Evaluation of QuantiFERON SARS-CoV-2 and QIAreach Anti-SARS-
459 CoV-2 Total Test in Recently Vaccinated Individuals. Infect Dis Ther. 2021;10: 2765–
460 2776. doi:10.1007/S40121-021-00521-8
461 37. Yoshida S, Ono C, Hayashi H, Fukumoto S, Shiraishi S, Tomono K, et al. SARS-
462 CoV-2-induced humoral immunity through B cell epitope analysis in COVID-19
463 infected individuals. Scientific Reports 2021 11:1. 2021;11: 1–13.
464 doi:10.1038/s41598-021-85202-9
465 38. Pedregosa FABIANPEDREGOSA F, Michel V, Grisel OLIVIERGRISEL O, Blondel
466 M, Prettenhofer P, Weiss R, et al. Scikit-learn: Machine Learning in Python Gaël
467 Varoquaux Bertrand Thirion Vincent Dubourg Alexandre Passos PEDREGOSA,
468 VAROQUAUX, GRAMFORT ET AL. Matthieu Perrot. Journal of Machine Learning
469 Research. 2011;12: 2825–2830. Available: http://scikit-learn.sourceforge.net.
470 39. Wolock SL, Lopez R, Klein AM. Scrublet: Computational Identification of Cell
471 Doublets in Single-Cell Transcriptomic Data. Cell Syst. 2019;8: 281-291.e9.
472 doi:10.1016/J.CELS.2018.11.005
473 40. Le T, Phan T, Pham M, Tran D, Lam L, Nguyen T, et al. BBrowser: Making single-
474 cell data easily accessible. bioRxiv. 2020; 2020.12.11.414136.
475 doi:10.1101/2020.12.11.414136
476 41. Kaech SM, Wherry EJ, Ahmed R. Effector and memory T-cell differentiation:
477 implications for vaccine development. Nature Reviews Immunology 2002 2:4. 2002;2:
478 251–262. doi:10.1038/nri778
479 42. Sallusto F, Geginat J, Lanzavecchia A. Central Memory and Effector Memory T Cell
480 Subsets: Function, Generation, and Maintenance. Annu Rev Immunol. 2004;22: 745–
481 763. doi:10.1146/ANNUREV.IMMUNOL.22.012703.104702
482 43. Wang Y, Chen Z, Wang T, Guo H, Liu Y, Dang N, et al. A novel CD4+ CTL subtype
483 characterized by chemotaxis and inflammation is involved in the pathogenesis of
484 Graves' orbitopathy. Cellular & Molecular Immunology 2021 18:3. 2021;18: 735–745.
485 doi:10.1038/s41423-020-00615-2
486 44. Matsumoto Y, Kishida K, Matsumoto M, Matsuoka S, Kohyama M, Suenaga T, et al.
487 A TCR-like antibody against a proinsulin-containing fusion peptide ameliorates type 1
488 diabetes in NOD mice. Biochem Biophys Res Commun. 2021;534: 680–686.
489 doi:10.1016/j.bbrc.2020.11.019

45. Kanda T, Miyata M, Kano M, Kondo S, Yoshizaki T, Iizasa H. Clustered MicroRNAs of the Epstein-Barr Virus Cooperatively Downregulate an Epithelial Cell-Specific Metastasis Suppressor. J Virol. 2015;89: 2684–2697. doi:10.1128/jvi.03189-14

46. Jiang Y, Arase N, Kohyama M, Hirayasu K, Suenaga T, Jin H, et al. Transport of misfolded endoplasmic reticulum proteins to the cell surface by MHC class II molecules. Int Immunol. 2013;25: 235–246. doi:10.1093/intimm/dxs155

Tables

Table 1. Demographic data of the participants.

	Percentage (number)
Total number	100% (43)
Age group	
20-39	39.5% (17)
40-49	30.2% (13)
50-59	25.6% (11)
60-69	4.7% (2)
Gender	
Male	60.5% (26)
Female	39.5% (17)

Table 2. Demographic data of the reported clinical adverse effects (at injection site)

	Percentage (number)
Swelling (injection site)	
After 1st dose	27.9% (12)
After 2nd dose	51.2% (22)
Sore/pain (injection site)	
After 1st dose	88.4% (38)
After 2nd dose	86.0% (37)
Warmth (injection site)	
After 1st dose	32.6% (14)
After 2nd dose	41.9% (18)

Table 3. Demographic data of the reported clinical adverse effects (systemic symptoms)

	Percentage (number)
Fever	
After 1st dose	
Mild (37.5°C ≥)	2.3% (1)
Severe (≥ 38.0°C)	0% (0)
After 2nd dose	
Mild (37.5°C ≥)	25.6% (11)
Severe (≥ 38.0°C)	23.3% (10)
Fatigue	
After 1st dose	
Mild	18.6% (8)
Severe	0% (0)
After 2nd dose	
Mild	67.4% (29)
Severe	18.6% (8)
Headache	
After 1st dose	
Mild	7.0% (3)
Severe	0% (0)
After 2nd dose	
Mild	32.6% (14)
Severe	7.0% (3)
Chill	
After 1st dose	
Mild	4.7% (2)
Severe	0% (0)
After 2nd dose	
Mild	23.3% (10)
Severe	9.3% (4)
Nausea	
After 1st dose	
Mild	0% (0)
Severe	0% (0)
After 2nd dose	
Mild	4.7% (2)
Severe	0% (0)
Diarrhea	
After 1st dose	
Mild	0% (0)
Severe	0% (0)
After 2nd dose	
Mild	0% (0)
Severe	0% (0)
Muscle pain	
After 1st dose	
Mild	48.8% (21)
Severe	0% (0)
After 2nd dose	
Mild	55.8% (24)
Severe	4.7% (2)
Joint pain	
After 1st dose	
Mild	4.7% (2)
Severe	0% (0)
After 2nd dose	
Mild	25.6% (11)
Severe	4.7% (2)

Table 4. TCR clonotypes expanded in post-vaccinated samples and their TCR usages, epitopes and restricting HLAs.

Donor	Clonotype	TRBV	CDR3β	TRBJ	TRAV	CDR3α	TRAJ	S epitope[a]	Restricting HLA
#8	Post_4	11-2	CASSPTGTNEKLFF	1-4	13-1	CAGGADGLTF	45	SFSTFKCYGVSPTKL$_{373–387}$[b]	DRA-DRB1*15:02
	Post_5	19	CASSGRPEGPQHF	1-5	20	CAVLNQAGTALIF	15	FKIYSKHTPIN$_{201–211}$	DRA-DRB1*09:01
	Post_6	11-2	CASSLEGTEAFF	1-1	5	CAESRYMGRRALTF	5	FQFCNDPFLGVYYHK$_{133–147}$	DPA1*01:03-DPB1*04:02
	Post_7	2	CAGLAGVDTGELFF	2-2	5	CAERVGRRALTF	5	YSVLYNSASFSTFKC$_{365–379}$	A*24:02
	Post_8	20-1	CSATRDRRSYNEQFF	2-1	12-2	CAVLTNTGNQFYF	49	LLQYGSFCTQLNRAL$_{753–767}$	DRA-DRB1*15:02
	Post_9	7-9	CASSLLGEQYF	2-7	22	CAGAGGTSYGKLTF	52	KRFDNPVLPFN$_{77–87}$	DPA1*02:02-DPB1*05:01
	Post_10	6-1	CASSEGASNQPQHF	1-5	12-1	CVVNKGSSASKIIF	3	LLQYGSFCTQL$_{753–763}$	DRA-DRB1*15:02
	Post_12	20-1	CSAYSIYNEQFF	2-1	9-2	CALSMNTGFQKLVF	8	PPAYTNSFTRGVYYP$_{25–39}$	DRA-DRB1*09:01
	Post_14	19	CASRPNRGDNSPLHF	1-6	12-1	CVVSIGFGNVLHC	35	CSNLLLQYGSFCTQL$_{749–763}$	DRA-DRB1*15:02
	Post_15	28	CASSLMGGAYGYTF	1-2	8-6	CAVRRGGSGGSNYKLTF	53	SKRSFIEDLLFNKVT$_{813–827}$	DPA1*01:03-DPB1*04:02
#25	Post_7	7-9	CAPSNANTGELFF	2-2	12-1	CVVNEADKLIF	34	YLQPRTFLLK$_{269–278}$	A*02:01
	Post_12	20-1	CSARDVEVGSGYTF	1-2	4	CLVGPYNQGGKLIF	23	TGVLTESNKKFLPFQ$_{549–563}$	DRA-DRB1*14:54
	Post_15	3-1	CASSPLSGSSYEQYF	2-7	12-1	CVVGTDSWGKLQF	24	TNGTKRFDNPVLPFN$_{73–87}$	DPA1*02:02-DPB1*05:01/ DPA1*01:03-DPB1*05:01
#27	Post_1	20-1	CSAIAGDADTQYF	2-3	9-2	CALTSAAGNKLTF	17	NQFNSAIGKIQ$_{925–935}$	DRA-DRB1*09:01
	Post_2	30	CAWNLGGGNQPQHF	1-5	8-2	CVVSERASSYKLIF	12	SKRSFIEDLLFNKVT$_{813–827}$	DPA1*02:02-DPB1*04:02
	Post_3	5-4	CASSQGQGSYGYTF	1-2	4	CLVGDSDTGRRALTF	5	NFTISVTTEIL$_{717–727}$	DRA-DRB1*09:01
	Post_5	7-2	CASGTGSYNEQFF	2-1	12-2	CAVKRGNQGGKLIF	23	STEIYQAGSTPCNGV$_{469–483}$	DRA-DRB1*04:03
	Post_7	6-6	CASRLPGNRAQPQHF	1-5	36/DV7	CAVESGSSNTGKLIF	37	KSNIIRGWIFGTTLD$_{97–111}$	DRA-DRB4*01:03
	Post_8	6-5	CASSYSGGTVTGELFF	2-2	41	CAVGIRGNEKLTF	48	KVFRSSVLHST$_{41–51}$	DRA-DRB1*04:03
	Post_9	20-1	CSARDGQTATNEKLFF	1-4	17	CATNAGGTSYGKLTF	52	EIRASANLAAT$_{1017–1027}$	DRA-DRB1*04:03
	Post_11	30	CAWSVKGFPSQHF	1-5	6	CALGSTSNTGKLIF	37	EIRASANLAAT$_{1017–1027}$	DRA-DRB1*04:03
	Post_13	5-6	CASSSRTGYNSPLHF	1-6	27	CAGAKGSGTYKYIF	40	STEIYQAGSTPCNGV$_{469–483}$	DRA-DRB1*04:03
	Post_15	5-5	CASSSDRNYGYTF	1-2	12-1	CVVNMVTGGYNKLIF	4	NFTISVTTEILPVSM$_{717–731}$	DRA-DRB1*09:01
	Post_16	7-9	CASSSQPGLAGVKIGNEQFF	2-1	5	CAEIPPPSNTGKLIF	37	ISGINASVVNIQKEI$_{1169–1183}$	DRA-DRB1*04:03
#28	Post_5	3-1	CASSQGGSEKLFF	1-4	1-1	CAVGGNTDKLIF	34	LVKNKCVNFNF$_{533–543}$	DRA-DRB3*03:01
	Post_10	12-3	CASSSGRTGFGYTF	1-2	30	CGTEFGSEKLVF	57	VIRGDEVRQIA$_{401–411}$	DRA-DRB3*03:01
	Post_11	5-8	CASSLQKTTGPSYGYTF	1-2	8-6	CAVSPYTGRRALTF	5	SVYAWNRKRIS$_{349–359}$	DRA-DRB1*13:02
	Post_12	18	CASSASVDPTEAFF	1-1	1-1	CASFTGGGNKLTF	10	KSTNLVKNKCVNFNF$_{529–543}$	DRA-DRB3*03:01
	Post_14	7-6	CASSLSGTGGTGELFF	2-2	4	CLVGDMRSGGGADGLTF	45	PFGEVFNATRFASVY$_{337–351}$	B*40:01
	Post_15	6-2	CASSYPPSGGRTGFGEAFF	1-1	14/DV4	CAMRDIGFGNVLHC	35	WNRKRISNCVADYSV$_{353–367}$	DRA-DRB4*01:03

[a]Overlapped epitope sequence is shown when a clonotype recognized two or three sequential peptides.
[b]Number ranges indicate the location of peptides in the proteins.

Table 4. Continued.

Donor	Clonotype	TRBV	CDR3β	TRBJ	TRAV	CDR3α	TRAJ	S epitope	Restricting HLA
#4	Post_2	25-1	CASTGDNYGYTF	1-2	21	CAINTGNQFYF	49	YYVGYLQPR$_{265–273}$	A*33:03
	Post_10	7-9	CASRPSGTSREQYF	2-7	29	CAGNNAGNMLTF	39	FIKQYGDCLGDIAAR$_{833–847}$	A*33:03
	Post_11	7-9	CASSTRTSGGGLSYEQYF	2-7	3	CAVNKAAGNKLTF	17	YSVLYNSASFSTFKC$_{365–379}$	A*24:02
	Post_13	20-1	CSASIEQGDLGYTF	1-2	23/DV6	CAASIPNSGYALNF	41	FIKQYGDCLGDIAAR$_{833–847}$	DQA1*01:02-DQB1*05:03
	Post_14	5-6	CASSPGQGILEQYF	2-7	24	CAFVPLSDGQKLLF	16	YIKWPWYIWL$_{1209–1218}$	A*24:02
	Post_15	7-3	CASGIHTGELFF	2-2	26-1	CIVNNAGNMLTF	39	TDNTFVSGNCDVVIG$_{1117–1131}$	DQA1*01:02-DQB1*06:04
	Post_16	7-6	CASSPGPSEADTQYF	2-3	1-1	CAVRDGDDKIIF	30	KSTNLVKNKCVNFNF$_{529–543}$	DRA-DRB3*03:01
#13	Post_13	7-2	CASSVGQSKGKSAETQYF	2-5	22	CAVNEYSGAGSYQLTF	28	SKRSFIEDLLFNKVT$_{813–827}$	DPA1*01:03-DPB1*02:01
	Post_15	20-1	CSAGDTASTYGYTF	1-2	9-2	CALSDGAGNKLTF	17	NQFNSAIGKIQ$_{925–935}$	DRA-DRB1*09:01
	Post_16	30	CAWSLQGQRPQHF	1-5	38-1	CAFMKQRGGSEKLVF	57	FIEDLLFNKVTLADA$_{817–831}$	DPA1*01:03-DPB1*02:01
#15	Post_1	12-4	CASSSHRDRGVEAFF	1-1	12-1	CVVNFDRGSTLGRLYF	18	TRGVYYPDKVF$_{33–43}$	B*15:01
	Post_6	3-1	CASSQQLNTGELFF	2-2	38-2/DV8	CAYRKTSGTYKYIF	40	WRVYSTGSNVF$_{633–643}$	DRA-DRB1*15:02
	Post_7	28	CASSFPDRYYSNQPQHF	1-5	1-2	CAVRAVGGNKLVF	47	TRGVYYPDKVF$_{33–43}$	B*15:01
	Post_9	27	CASSPGHEQYF	2-7	14/DV4	CAMSPIRTYKYIF	40	RSVASQSIIAY$_{685–695}$	B*15:01
	Post_11	3-1	CASSRELISEQYF	2-7	38-2/DV8	CAYKRTSGTYKYIF	40	WRVYSTGSNVF$_{633–643}$	DRA-DRB1*15:02
	Post_12	28	CASSSYGTSGGRAEQFF	2-1	16	CALSGGLTGGGNKLTF	10	LGDIAARDLICAQKF$_{841–855}$	DRA-DRB1*08:02
	Post_13	30	CAWRTGQGITSPLHF	1-6	8-2	CVVNNAGNMLTF	39	VFKNIDGYFKIYSKH$_{193–207}$	DPA1*02:02-DPB1*05:01
	Post_14	6-1	CASSEAGGSGANVLTF	2-6	9-2	CALSGTGTYKYIF	40	KKFLPFQQFGR$_{557–567}$	DPA1*02:02-DPB1*05:01
	Post_16	27	CASSLGTINTGELFF	2-2	17	CATAPAGGTSYGKLTF	52	IDGYFKIYSKHTPIN$_{197–211}$	DRA-DRB1*08:02
#17	Post_4	6-2	CASTSTARGSYNEQFF	2-1	27	CAGHSNTGNQFYF	49	TRFASVYAWNRKRIS$_{345–359}$	DRA-DRB1*08:02
	Post_10	9	CASSKTSGAYNEQFF	2-1	9-2	CALDNARLMF	31	FIKQYGD$_{833–839}$	DRA-DRB1*15:01
	Post_11	20-1	CSARPPGGGNNEQFF	2-1	26-2	CILRDGTGANNLFF	36	QALNTLVKQLSSNFG$_{957–971}$	DRA-DRB1*08:02
	Post_15	7-9	CASSLARGNSPLHF	1-6	38-2/DV8	CAFVGSQGNLIF	42	AARDLICAQKFNGLT$_{845–859}$	DRA-DRB1*08:02

Table 5. Reactivity of each clonotype to mutated epitopes in SARS-CoV-2 VOCs.

Donor	Clonotype	Mutated epitopes in VOCs		Domain	Response
#8	Post_4	Omicron BA.1 Omicron BA.2, 4/5	PFFTFKCYGVSPTKL[a] PFFAFKCYGVSPTKL	RBD	↓ ↓
#8	Post_5	Omicron BA.1	FKIYSKHTPII	non-RBD	↑
#8	Post_6	Delta, Omicron BA.2, 4/5 Omicron BA.1	FQFCNDPFLDVYYHK FQFCNDPFLD---HK	non-RBD	↓ ↓
#8	Post_7	Omicron BA.1 Omicron BA.2, 4/5	YSVLYNLAPFFTFKC YSVLYNFAPFFAFKC	RBD	↓ ↓
#8	Post_8	Omicron BA1, 2, 4/5	LLQYGSFCTQLKRAL	non-RBD	↑
#8	Post_10	Omicron BA1, 2, 4/5	LLQYGSFCTQLKRAL	non-RBD	↑
#27	Post_5	Delta Omicron BA.1, 2, 4/5	STEIYQAGSKPCNGV STEIYQAGNKPCNGV	RBD	↓ ↓
#27	Post_13	Delta Omicron BA.1, 2, 4/5	STEIYQAGSKPCNGV STEIYQAGNKPCNGV	RBD	↓ ↓
#28	Post_5	Omicron BA.1	LVKNKCVNFNFNGLK	non-RBD	↑
#28	Post_10	Omicron BA.2, 4/5	VIRGNEVSQIA	RBD	↓
#28	Post_14	Omicron BA.1, 2, 4/5	PFDEVFNATRFASVY	RBD	↓
#4	Post_11	Omicron BA.1 Omicron BA.2, 4/5	YSVLYNLAPFFTFKC YSVLYNFAPFFAFKC	RBD	↓ ↓
#15	Post_9	Delta Omicron BA.1, 2, 4/5	RRRARSVASQSIIAY HRRARSVASQSIIAY	non-RBD	↑ ↑
#15	Post_16	Omicron BA.1	IDGYFKIYSKHTPII	non-RBD	→
#17	Post_11	Omicron BA.1, 2, 4/5	QALNTLVKQLSSKFG	non-RBD	↓
#17	Post_15	Omicron BA.1	AARDLICAQKFKGLT	non-RBD	↓

[a]Amino acids colored red indicate mismatches compared with corresponding S epitopes of Wuhan strain.

Table 6. S-cross-reactive TCR clonotypes expanded in pre-vaccinated samples and their TCR usages, epitopes, restricting HLAs and cross-reactive epitopes in microbes other than SARS-CoV-2.

Donor	Clonotype	TRBV	CDR3β	TRBJ	TRAV	CDR3α	TRAJ	S epitope	Restricting HLA	Cross-reactive antigen [species]	Cross-reactive peptide	Post-vaccinated expansion
#4	Pre_5	6-6	CASSYPGGGGSETQYF	2-5	35	CAGVAVQGAQKLVF	54	LLALHRSYLTP$_{241–251}$[a]	DRA-DRB1*14:54	Phosphoribosylformylglycinamidine cyclo-ligase [*Firmicutes bacterium*]	VAEALLAVHRSYLTP$_{220-234}$[b]	No
#4	Pre_7	6-6	CASSYPGGSGGELFF	2-2	21	CAVENSGNTPLVF	29	LLALHRSYLTP$_{241–251}$	DQA1*01:04-DQB1*05:03	Phosphoribosylformylglycinamidine cyclo-ligase [*Firmicutes bacterium*]	VAEALLAVHRSYLTP$_{220-234}$	No
#8	Pre_1	6-2	CASRPNRGRFRGNQPQHF	1-5	23/DV6	CAGEEKETSGSRLTF	58	NCTFEYVSQPFLMDL$_{165–179}$	DRA-DRB1*15:01	Fumarylacetoacetate hydrolase family protein [*Alcaligenes faecalis*] Hypothetical protein [*Planctomycetales bacterium*]	ASLIEYVSQPFLLEP$_{225-239}$ AAGFEYVSQPFSLPL$_{533-547}$	No
#8	Pre_2	6-1	CASIRDRVADTQYF	2-3	30	CGTETTDSWGKLQF	24	RFNGIGVTQNV$_{905–915}$	DQA1*03:02-DQB1*03:03	SEL1-like repeat protein [*Bacteroidaceae bacterium*][c]	LGVYYFNGIGVTQDQ$_{236-250}$	No
#8	Pre_3	27	CATKGEANYGYTF	1-2	12-3	CAMSEMGTGFQKLVF	8	SIVRFPNITNL$_{325–335}$	DRA-DRB1*15:01	LTA synthase family protein [*Dechloromonas denitrificans*]	LPGKSVVRWPNITNL$_{330-344}$	No
#8	Pre_5	5-1	CASSLRTGELFF	2-2	8-1	CAVNGRNTGFQKLVF	8	NFTISVTTEILPVSM$_{717–731}$	DRA-DRB1*09:01	Major capsid protein [*Human papillomavirus 145*] Periplasmic trehalase [*Chlamydiia bacterium*]	NFTISVTTDAGDINE$_{350-364}$ LSTIVTTEILPVDL$_{288-301}$	No
#8	Pre_9	7-2	CASAAGGTGGETQYF	2-5	5	CAETPFLSGTYKYIF	40	YIKWPWYIWLGFIAG$_{1209–1223}$	DRA-DRB5*01:02	Spike glycoprotein [*Human coronavirus HKU1*]	VKWPWYVWLLISFSF$_{1297-1311}$	No
#8	Pre_10	6-6	CASSLGQGIHEQYF	2-7	26-1	CIVERGGSNYKLTF	53	SKRSFIEDLLFNKVT$_{813–827}$	DPA1*01:03-DPB1*04:02	Hypothetical protein, partial [*Acinetobacter baumannii*] Spike protein [*Feline coronavirus*] Spike protein [*Canine coronavirus*]	GKRSAVEDLLFNKVV$_{204-218}$ GKRSAVEDLLFNKVV$_{980-994}$ GKRSAVEDLLFNKVV$_{977-991}$	No
#8	Pre_14	4-3	CASSQRQGAGDTQYF	2-3	19	CALSEAGIQGAQKLVF	54	IDRLITGRLQSLQTY$_{993–1007}$	DQA1*01:03-DQB1*06:01	Excinuclease ABC subunit UvrA [*Lentisphaeria bacterium*]	VDRLITGRLESSRLN$_{208-222}$	No
#8	Pre_15	20-1	CSAKDRIYGYTF	1-2	26-1	CIVRSPSGSARQLTF	22	MIAQYTSALLA$_{869–879}$	DRA-DRB1*15:01	MATE family efflux transporter [*Selenomonas noxia*]	ATIIAQYTSALLALR$_{242-256}$	No
#13	Pre_5	4-3	CASSQVSTGTGITGANVLTF	2-6	5	CARRSSSASKIIF	3	QNVLYENQKLI$_{913–923}$	DRA-DRB5*01:02	Hypothetical protein [*Neobacillus vireti*]	TNVLYENQKLFLNLF$_{169-183}$	No
#13	Pre_8	18	CASSPRAPPYEQYF	2-7	21	CAVRPAGGTGNQFYF	49	DKYFKNHTSPDVDLG$_{1153–1167}$	DRA-DRB1*15:01	Type VI secretion system contractile sheath large subunit [*Salmonella enterica*]	DYYFDHTSPDVDLLG$_{167-181}$	No
#13	Pre_12	4-2	CASSQEGNTEAFF	1-1	20	CGCRGGTSYGKLTF	52	NVTWFHAIHVSGTNG$_{61–75}$	A*02:07	Dihydrofolate synthase [*Actinobaculum sp. 313*]	PQRSFHAIHVTGTNG$_{61-75}$	No
#15	Pre_1	20-1	CSARDLTASAHGYTF	1-2	17	CATDAGQGGKLIF	23	SVTTEILPVSM$_{721–731}$	DQA1*01:03-DQB1*06:01	Hypothetical protein [*Myxococcales bacterium*]	PVTTEILPVSDDPPG$_{525-539}$	No
#15	Pre_2	24-1	CATSDLDQPQHF	1-5	16	CALSGYGSGYSTLTF	11	SVTTEILPVSM$_{721–731}$	DQA1*01:03-DQB1*06:01	Hypothetical protein [*Myxococcales bacterium*]	PVTTEILPVSDDPPG$_{525-539}$	No
#15	Pre_3	6-1	CASDPKNGGEQYF	2-7	29/DV5	CAASVGFGNVLHC	35	FKIYSKHTPIN$_{201–211}$	DRA-DRB5*01:02	Uncharacterized protein APUU_31289S [*Aspergillus puulaauensis*]	CRAAFKLYSKHTPVE$_{123-137}$	No
#15	Pre_4	19	CASGLAGGNTGELFF	2-2	10	CVPSSGGYNKLIF	4	QALNTLVKQLS$_{957–967}$	DRA-DRB1*08:02	4-hydroxybenzoate octaprenyltransferase [*Pseudoduganella dura*]	IQPLNTLVKQLSVAA$_{112-126}$	No
#15	Pre_5	6-5	CASSAGLAGGGNTQYF	2-3	5	CAVISGSARQLTF	22	QALNTLVKQLS$_{957–967}$	DRA-DRB1*08:02	4-hydroxybenzoate octaprenyltransferase [*Pseudoduganella dura*]	IQPLNTLVKQLSVAA$_{112-126}$	No
#15	Pre_6	2	CASVGGNEQFF	2-1	9-2	CALTRFVGGATNKLIF	32	RTFLLKYNENGTITD$_{273–287}$	DRA-DRB1*15:01	Unnamed protein product [*Mytilus edulis*]	NKKLLKYNENGTFIT$_{277-291}$	No
#15	Pre_7	4-1	CASSHDGTPPDTQYF	2-3	29/DV5	CAAYSNYQLIW	33	FKIYSKHTPIN$_{201–211}$	DRA-DRB1*15:01	Uncharacterized protein APUU_31289S [*Aspergillus puulaauensis*]	CRAAFKLYSKHTPVE$_{123-137}$	No
#15	Pre_15	2	CASSETGRGTDTQYF	2-3	9-2	CALYRGTYKYIF	40	LQSLQTYVTQQLIRA$_{1001–1015}$	DRA-DRB1*15:01	Dyp-type peroxidase [*Acinetobacter sp.*]	CTVLQTYVTQQLESV$_{134-148}$	No
#17	Pre_7	6-1	CASSLRGAFGYTF	1-2	35	CAGHLYGGSQGNLIF	42	NCTFEYVSQPFLMDL$_{165–179}$	DPA1*01:03-DPB1*04:02	Fumarylacetoacetate hydrolase family protein [*Alcaligenes faecalis*] Hypothetical protein [*Planctomycetales bacterium*]	ASLIEYVSQPFLLEP$_{225-239}$ AAGFEYVSQPFSLPL$_{533-547}$	No
#17	Pre_8	5-1	CASSLNSGANVLTF	2-6	13-1	CAASIVQDQKLVF	8	LTPTWRVYSTGSNVF$_{629–643}$	DRA-DRB1*08:02	Hypothetical protein [*Novosphingobium chloroacetimidivorans*]	APGTPTWRVYSTART$_{277-291}$	No
#17	Pre_14	5-1	CASSLGAGLYNEQFF	2-1	38-1	CAFINNNAGNMLTF	39	QALNTLVKQLS$_{957–967}$	DRA-DRB1*08:02	4-hydroxybenzoate octaprenyltransferase [*Pseudoduganella dura*]	IQPLNTLVKQLSVAA$_{112-126}$	No
#17	Pre_15	7-2	CASSRTSGGTYEQYF	2-7	25	CAGQNTDKLIF	34	SIVRFPNITNL$_{325–335}$	DRA-DRB1*15:01	LTA synthase family protein [*Dechloromonas denitrificans*]	LPGKSVVRWPNITNL$_{330-344}$	Yes

[a]Number ranges indicate the location of peptides in the proteins.
[b]Amino acids colored red indicate mismatches compared with corresponding S epitopes of Wuhan strain.
[c]Antigen names and peptide sequences in light gray indicate inactive antigens of the corresponding T clonotypes.

Fig. 1

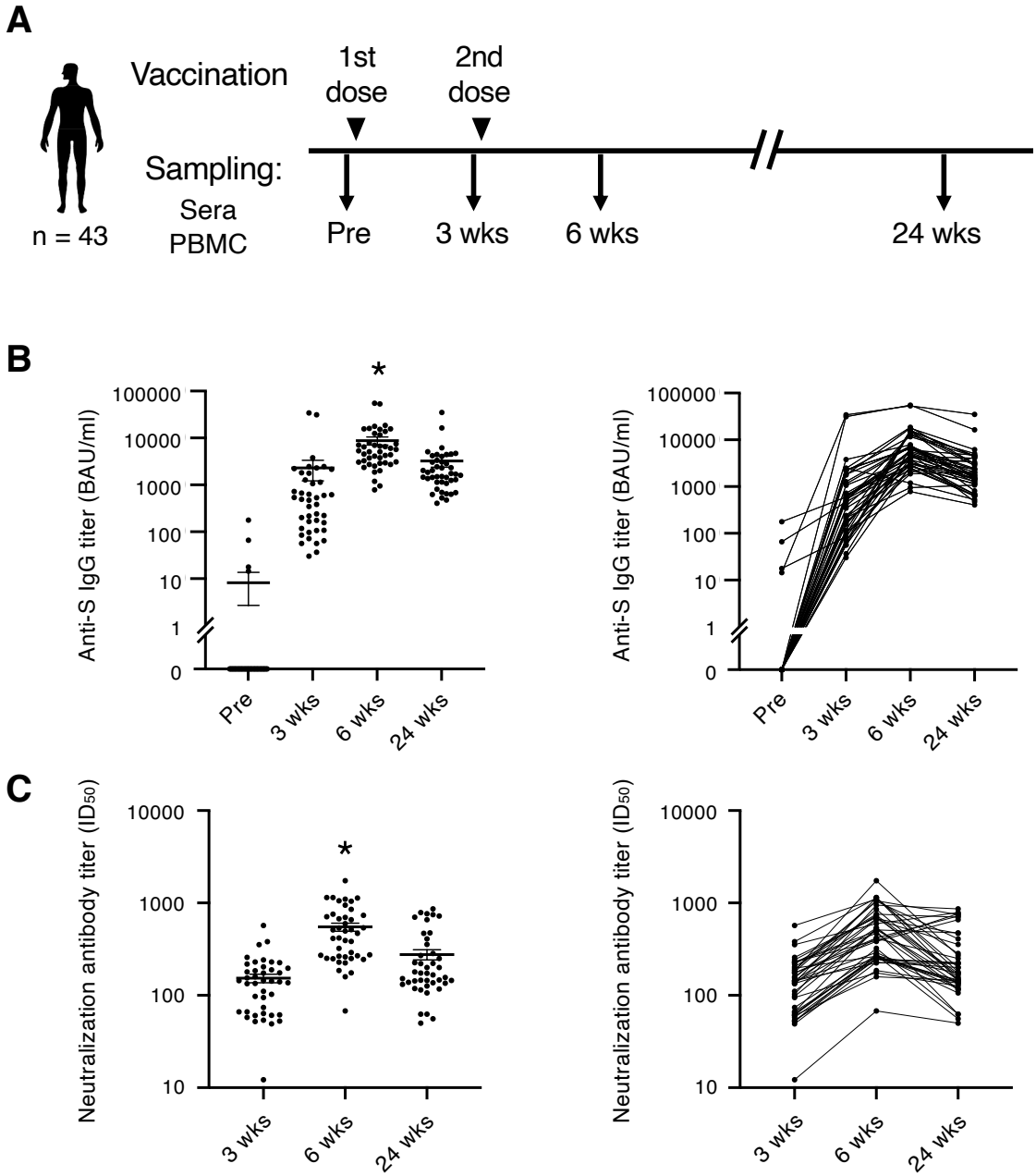

Fig. 1. SARS-CoV-2 mRNA vaccine elicits transient humoral immunity.

(**A**) Vaccination and sampling timeline of blood donors in this study. (**B**) Anti-S IgG titer of serum samples was determined by ELISA. Mean ± SEM (left) and individual data (right) are shown. *, $P < 0.05$ vs. Pre, 3 wks, 24 wks, respectively. (**C**) Neutralization activity (ID50) of serum samples was determined by pseudo-virus assay. Mean ± SEM (left) and individual data (right) are shown. *, $P < 0.05$ vs. 3 wks, 24 wks, respectively. Wks, weeks.

Fig. 2

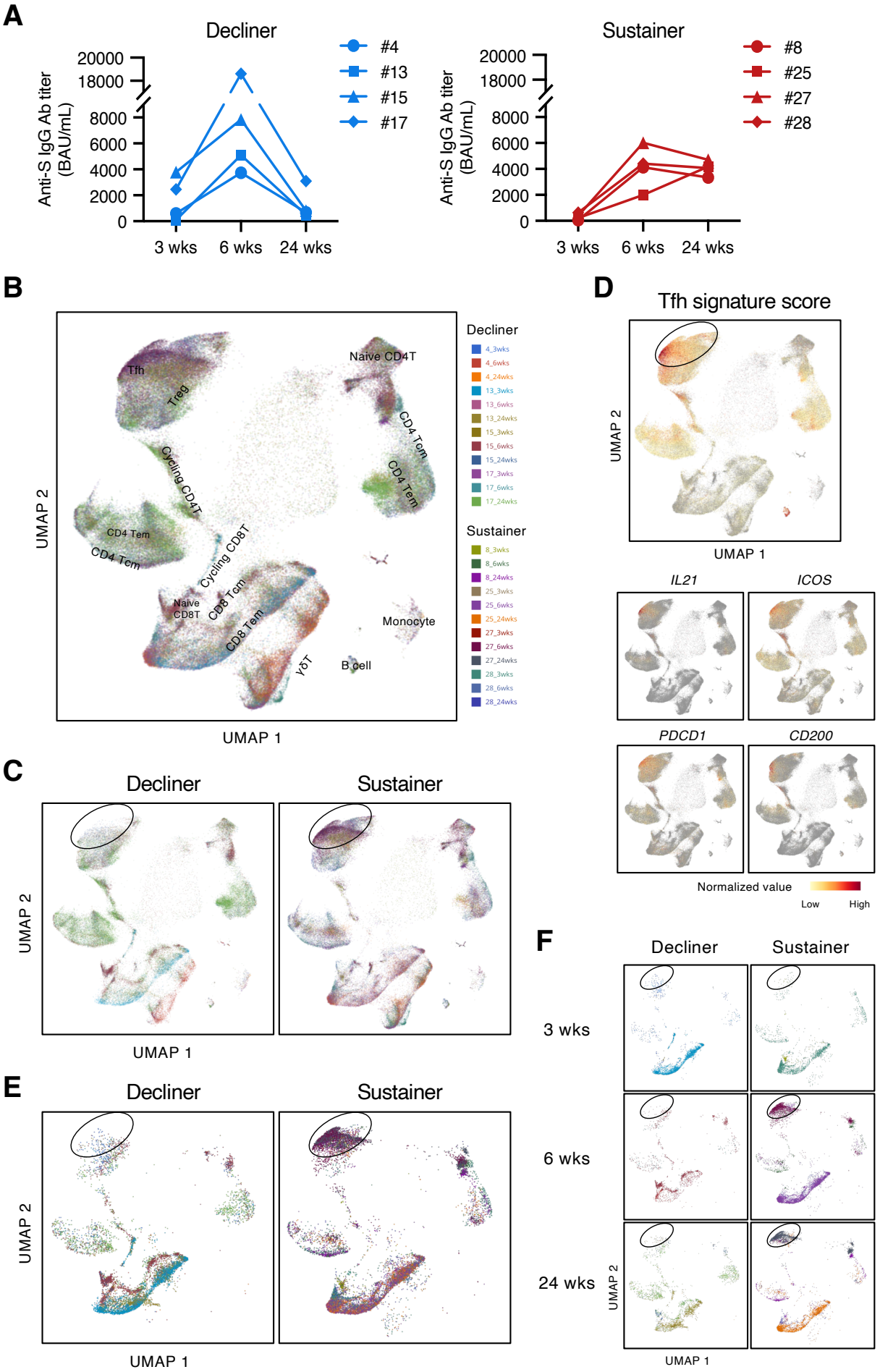
A
Decliner
Sustainer
Anti-S IgG Ab titer (BAU/mL)
20000
18000
8000
6000
4000
2000
0
3 wks
6 wks
24 wks
#4
#13
#15
#17
#8
#25
#27
#28
B
UMAP 1
UMAP 2
Tfh
Treg
Naive CD4T
CD4 Tcm
CD4 Tem
Cycling CD4T
Cycling CD8T
CD8 Tcm
CD8 Tem
Naive CD8T
γδT
B cell
Monocyte
Decliner
Sustainer
C
Decliner
Sustainer
D
Tfh signature score
IL21
ICOS
PDCD1
CD200
Normalized value
Low
High
E
F
3 wks
6 wks
24 wks

Fig. 2. Antibody sustainers had highly expanded S-reactive Tfh clonotypes.

(**A**) Anti-S IgG titer of serum samples from sustainers and decliners is shown individually. (**B, C, E,** and **F**) UMAP projection of T cells in single-cell analysis of post-vaccinated samples collected from all donors. Each dot corresponds to a single cell and is colored according to the samples from different time points of donors. All samples together with annotated cell types (B), samples grouped by donor type (decliners and sustainers) (C), top 16 expanded clonotypes (16 clonotypes that had the most cell numbers from each donor) grouped by donor type (E), and top 16 expanded clonotypes grouped by time point and donor type (F) are shown. Tcm, central memory T cells; Tem, effector memory T cells; Treg, regulatory T cells; γδT, γδ T cells. (**D**) Tfh signature score and expression levels of the canonical Tfh cell markers, *IL21*, *ICOS*, *PDCD1* and *CD200*, are shown as heat maps in the UMAP plot.

Fig. 3

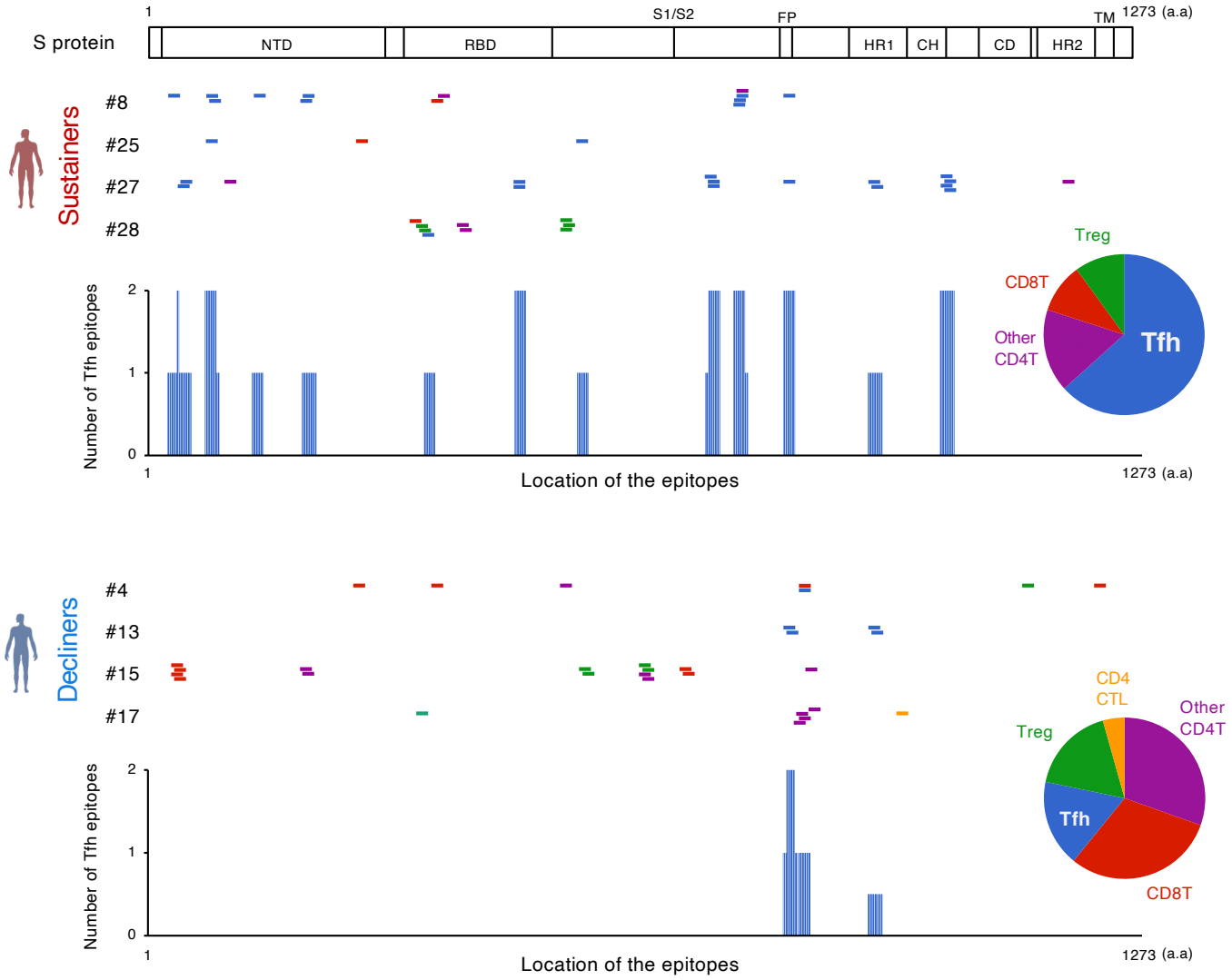

Fig. 3. The location of S epitopes recognized by top expanded T clonotypes from post-vaccination samples.

T cell S epitopes recognized by top expanded TCR clonotypes in post-vaccinated samples from sustainers and decliners are mapped by their locations in S protein. Each short bar indicates a 15-mer peptide that activated the TCRs. Epitopes are shown in different colors according to the subsets of the T cells they activated. Relative frequencies of the T cell subsets are shown in pie charts. Numbers of identified epitopes recognized by a dominant T subset in sustainers (Tfh) are shown in blue bars. NTD, N-terminal domain; RBD, receptor-binding domain; FP, fusion peptide; HR1, heptad repeat 1; CH, central helix; CD, connector domain; HR2, heptad repeat 2; TM, transmembrane domain.

Fig. 4

A

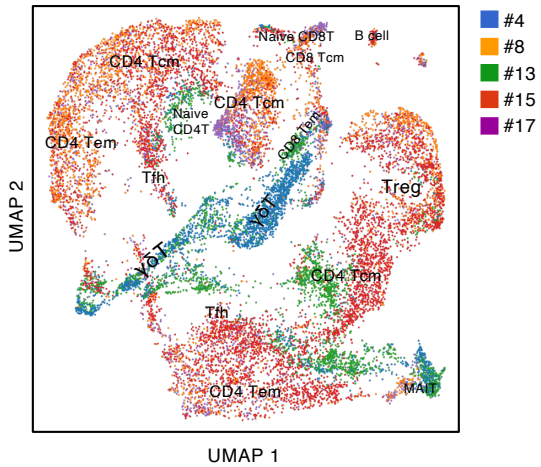

B

Clonotype fraction: Min – Max

Donor	Clonotype#	Cell type	Percentage in T cells (%)				Expansion
			Pre	3wks	6wks	24wks	Post(max) /Pre
#13	Post_8	CD4 Tem	7.67	0.65	0.00	0.62	0.08
#13	Pre_2	CD4 Tem	6.16	0.00	0.00	0.00	0.00
#13	Post_1	CD8 Tem	6.16	44.72	28.97	7.65	7.26
#4	Post_3	CD4 Tem	5.76	1.22	0.03	0.73	0.21
#13	Post_2	CD8 Tem	5.30	10.44	16.55	21.00	3.97
#13	Pre_1	MAIT	5.20	0.04	0.00	0.00	0.01
#15	Pre_1	CD4 Tem	3.24	0.00	0.00	0.00	0.00
#17	Pre_1	CD4 Treg	3.02	0.00	0.00	0.00	0.00
#13	Pre_3	CD4 Tcm	2.79	0.00	0.00	0.00	0.00
#15	Pre_2	CD4 Tem	2.77	0.20	0.25	0.00	0.09
#15	Pre_3	CD4 Tem	2.74	0.00	0.00	0.47	0.17
#15	Pre_4	CD4 Tcm/Treg	2.68	0.00	0.00	0.00	0.00
#4	Pre_1	CD8 Tem	2.45	0.18	0.06	0.00	0.07
#15	Pre_7	CD4 Tcm	2.36	0.00	0.00	0.07	0.03
#8	Pre_2	CD4 Tem	1.87	0.06	0.04	0.00	0.03
#8	Pre_1	CD4 Tcm/Treg	1.84	0.00	0.00	0.00	0.00
#8	Pre_4	CD4 Treg	1.84	0.13	0.00	0.00	0.07
#15	Pre_8	CD4 Tem	1.42	0.00	0.00	0.00	0.00
#15	Pre_14	CD4 Tfr	1.39	0.00	0.00	0.00	0.00
#15	Pre_5	CD4 Tem	1.31	0.00	0.07	0.15	0.11
#15	Pre_6	CD4 Tem	1.31	0.00	0.00	0.00	0.00
#15	Pre_12	CD4 Tcm/Treg	1.25	0.00	0.00	0.04	0.03
#15	Pre_10	CD4 Tem	1.19	0.20	0.19	0.00	0.17
#15	Pre_9	CD4 Treg	0.92	0.00	0.00	0.00	0.00
#15		CD4 Treg	0.92	0.00	0.00	0.00	0.00
#15	Pre_15	CD4 Tcm/Treg	0.89	0.00	0.04	0.00	0.04
#15	Pre_13	CD4 Tem	0.88	0.00	0.33	0.00	0.38
#8	Post_1	CD8 Tem	0.86	3.12	0.52	1.14	3.63
#15		CD4 Treg	0.80	0.00	0.16	0.15	0.19
#15		CD4 Treg	0.80	0.00	0.00	0.00	0.00
#15		CD4 Tem	0.77	0.00	0.00	0.00	0.00
#4	Post_1	CD8 Tem	0.61	0.77	3.69	2.18	6.02
#17		CD8 Tem	0.35	1.16	0.00	0.16	3.34
#17		CD8 Tem	0.30	0.00	0.00	0.21	0.69
#8		CD4 Tfr	0.28	0.42	1.19	0.00	4.31
#15	Post_3	CD4 CTL	0.22	2.76	2.35	1.31	12.80
#15	Post_8	CD4 CTL	0.22	1.18	0.87	0.47	5.49
#17	Post_2	CD8 Tem	0.20	0.80	0.21	0.77	4.02
#13	Post_3	CD8 Tem	0.16	1.21	0.69	0.05	7.52
#13	Post_5	CD8 Tem	0.13	1.03	2.07	0.11	16.12
#15		CD4 Tfr	0.11	1.18	0.25	0.73	10.97
#17		CD8 Tem	0.10	0.22	0.11	0.24	2.41
#15	Post_2	CD4 CTL/Treg	0.06	0.99	2.59	1.17	42.01
#8	Post_15	CD4 Treg->Tcm	0.06	0.17	0.00	1.73	28.14
#13	Post_6	CD8 Tem	0.03	1.30	0.69	0.27	40.39

Fig. 4. Characteristics and dynamics of S-cross-reactive clonotypes.
(**A**) UMAP projection of T cells in single-cell analysis of pre-vaccinated T cells from donors #4, #13, #15, #17, and #8. Each dot corresponds to a single cell and is colored according to the samples from different donors. Annotated cell types are shown. (**B**) Donor, name of reconstituted clonotypes, cell type, clonotype fraction in T cells from each time points, and expansion ratio of clonotypes that were found in pre-vaccinated samples and had more than 50 cells in the combined pre- and post-vaccinated sample set. For clonotypes that showed more than one type, the major type is listed in the front. The expansion ratio was calculated using the maximum cell fraction at post-vaccination points divided by the cell fraction at the pre-vaccination point of each clonotype. Clonotypes that have an expansion ratio larger than 1 are considered as expanded post-vaccination. Cell fractions at individual time points are shown as heat map. Tfr, follicular regulatory T cells; MAIT, mucosal-associated invariant T cells.

Fig. 5

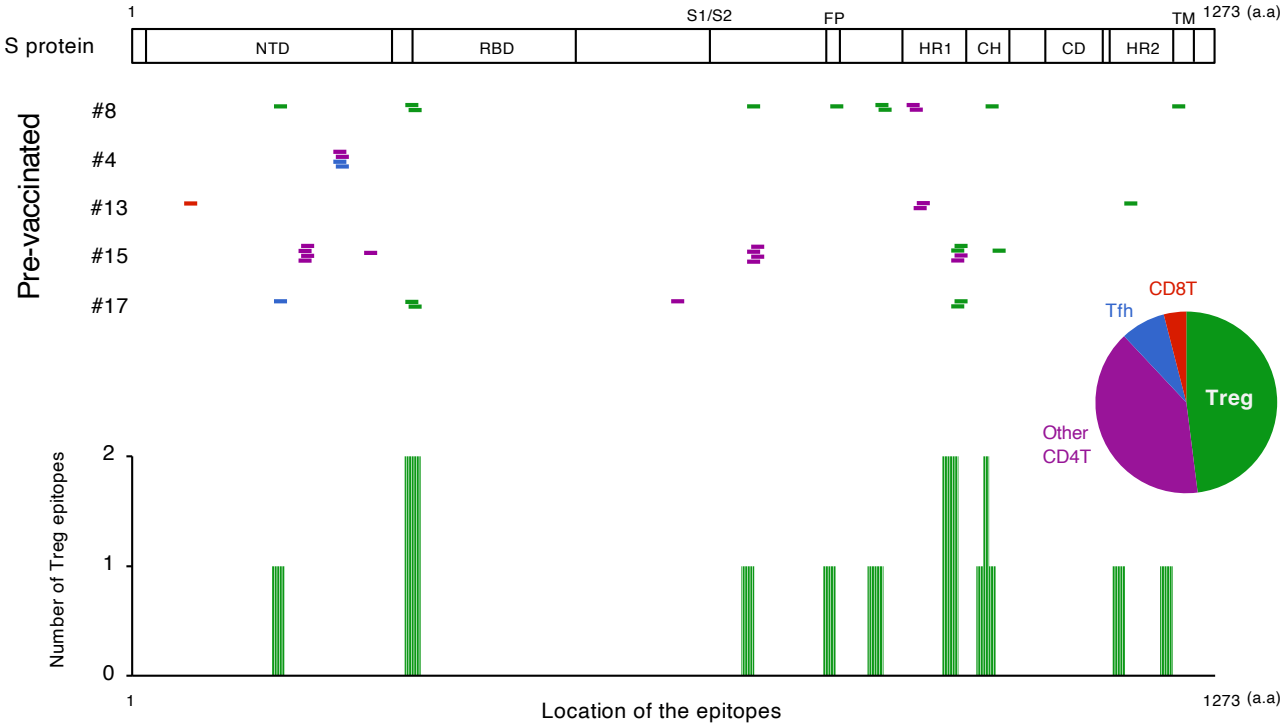

Fig. 5. The location of S epitopes of pre-existing S-reactive T cells.

S epitopes recognized by top expanded TCR clonotypes in pre-vaccinated samples are mapped by their locations in S protein. Each short bar indicates a 15-mer peptide that activated the TCRs. Epitopes are shown in different colors according to the subtypes of the T cells they activated. Relative frequencies of the T cell subtypes from all five donors are shown in the pie chart. Numbers of identified epitopes recognized by a dominant T subset of pre-existing clonotypes (Treg) from all donors are shown in green bars.

Fig. 6

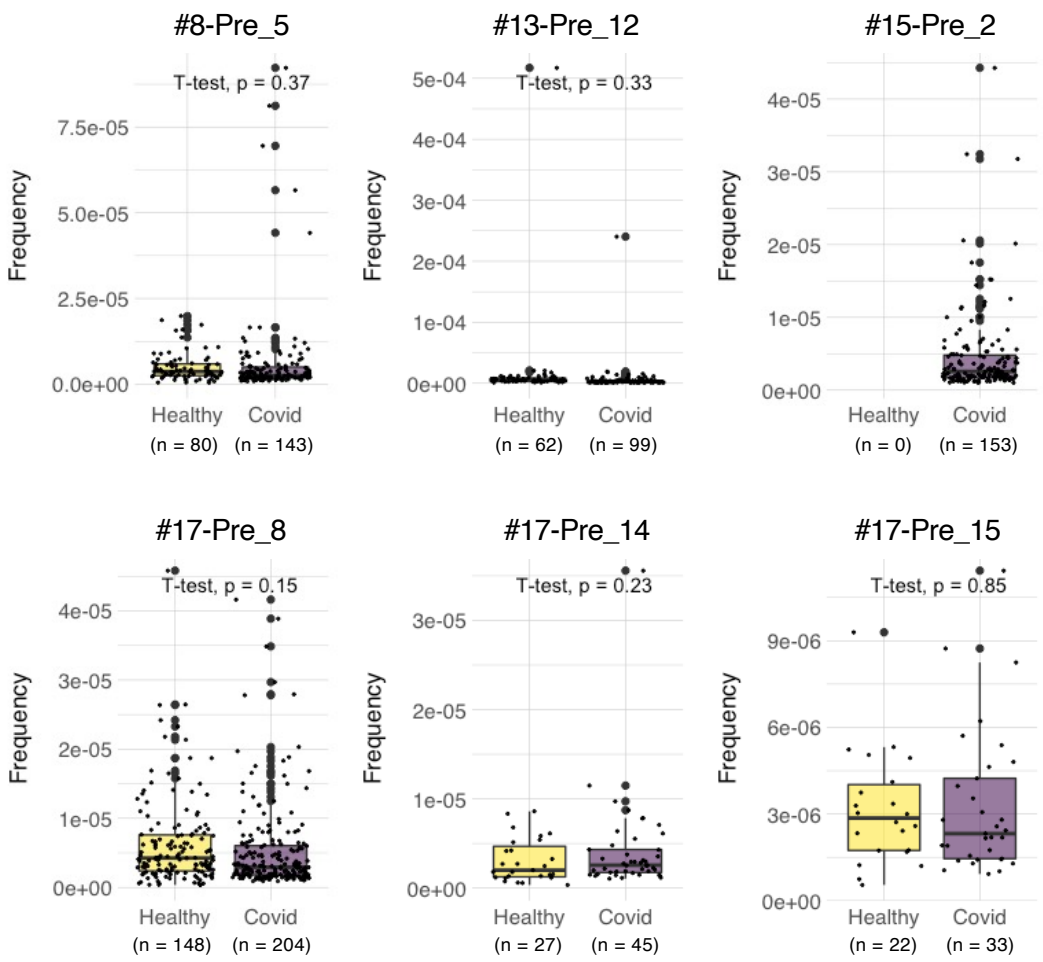

Fig. 6. Frequencies of pre-existing S-reactive clonotypes in the public database of uninfected and infected cohorts.

TCRβ sequences of the top expanded clonotypes in pre-vaccinated samples were investigated in the Adaptive database. Frequencies of detected clonotypes are shown in box plot. Healthy, dataset from 786 healthy donors. COVID, dataset from 1487 COVID-19 patients.

Fig. S1

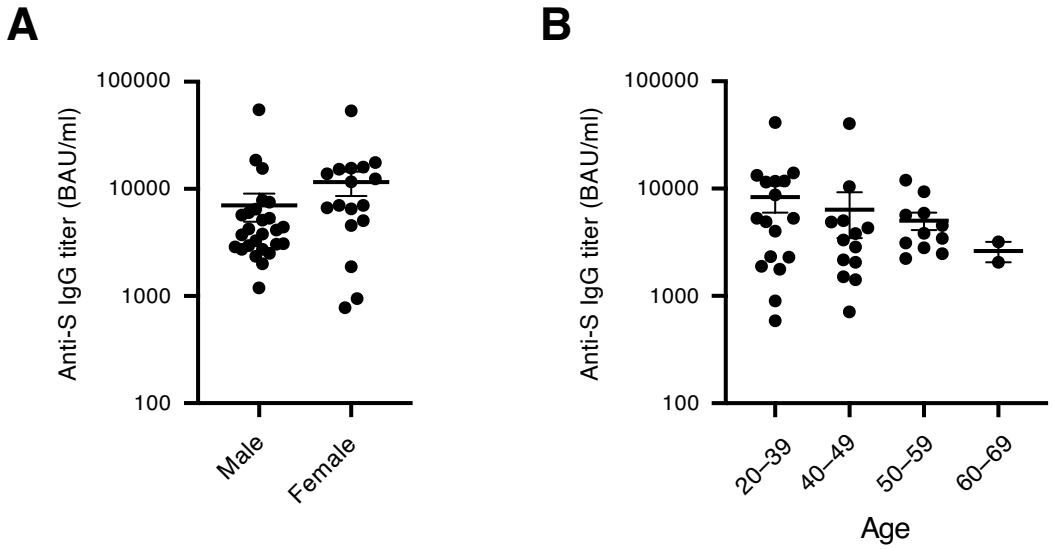

Fig. S1. Humoral immune response of BNT162b2 vaccinees.

(**A** and **B**) Anti-S IgG titer from all donors at 6 weeks after vaccination was compared between male and female vaccinees (A) or among different age groups (20–39, 40–49, 50–59, 60–69) (B).

Fig. S2

A

Donor	Age (years)	Gender	Anti-S IgG titer reduction (6 - 24 wks)
Sustainers	**(49 ± 5.2)**		
#8	55	male	18.8%
#25	47	male	-108.7%
#27	51	male	21.6%
#28	43	male	7.7%
Decliner	**(48.5 ± 10.8)**		
#4	51	male	81.8%
#13	58	male	90.7%
#15	52	male	89.6%
#17	33	male	83.4%

B

Sample	Anti-N IgG titer (OD_{50})
#8	0.0
#25	1.2
#27	0.0
#28	1.3
Convalescent 1	187.6
Convalescent 2	68.5
WHO STD 20/136	225.8

C

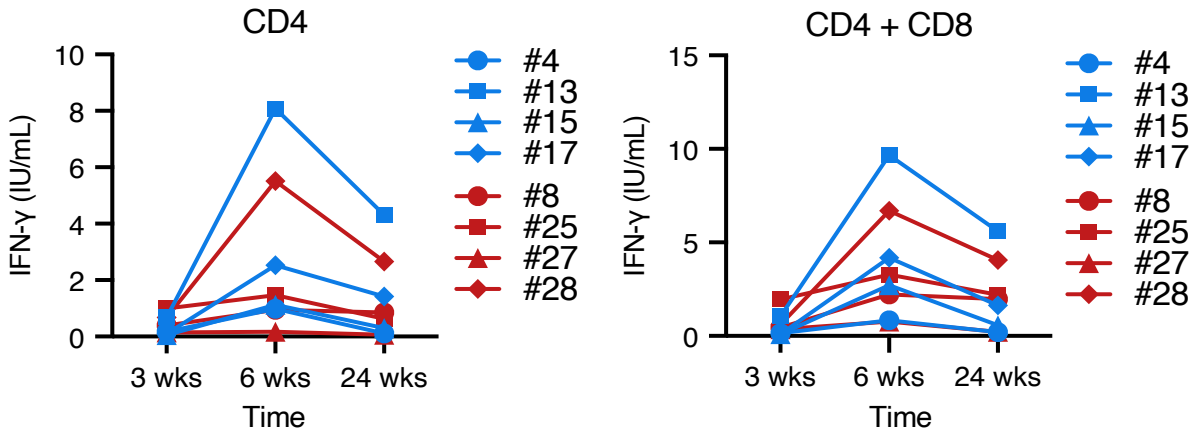

Fig. S2. Humoral and cellular immune responses of sustainers and decliners.

(**A**) Demographic data and magnitude of anti-S IgG titer reduction of the sustainers and decliners. Anti-S IgG titer reduction is calculated as the titers at (6 wks – 24 wks) /6 wks. (**B**) Anti-N IgG titer of serum samples from sustainers at 24 weeks after vaccination. (**C**) S-specific IFNγ release from bulk $CD4^+$ T cells (left) or $CD4^+$ and $CD8^+$ T cells (right) of sustainers (red) and decliners (blue) was measured using QuantiFERON.

Fig. S3

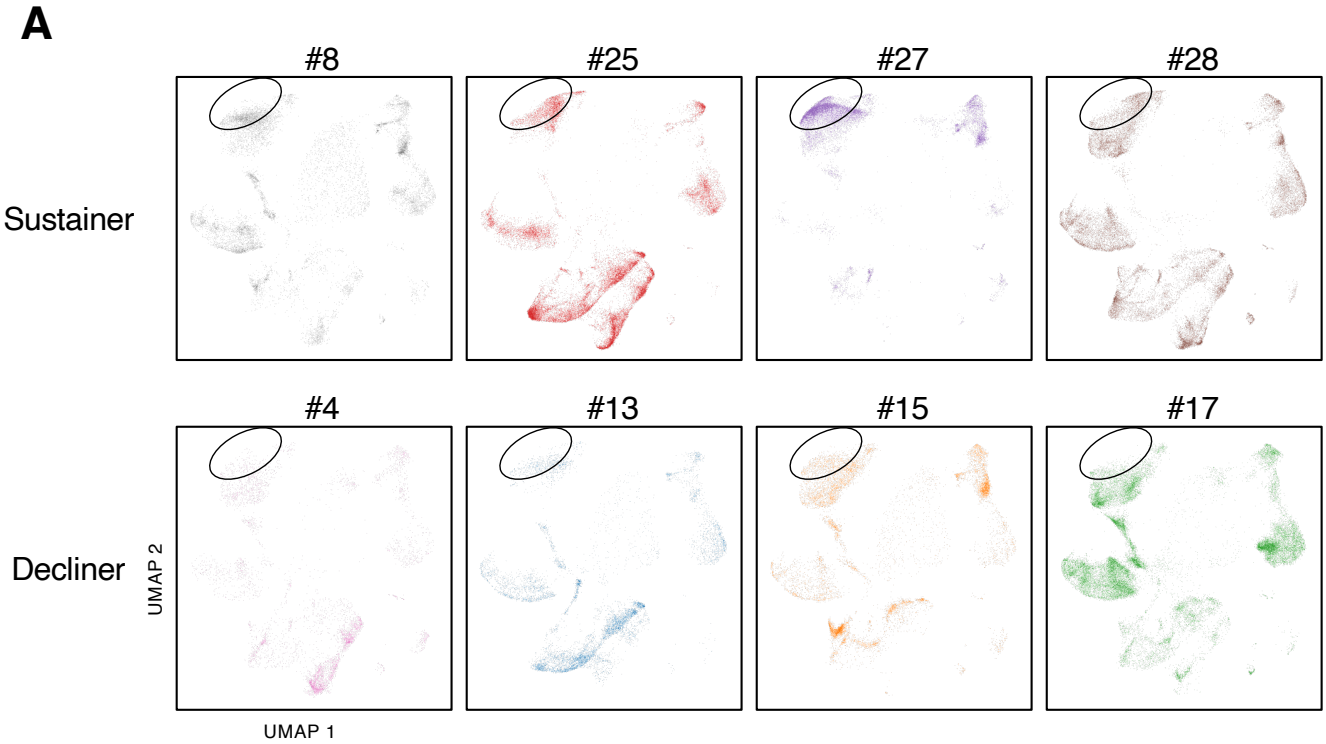

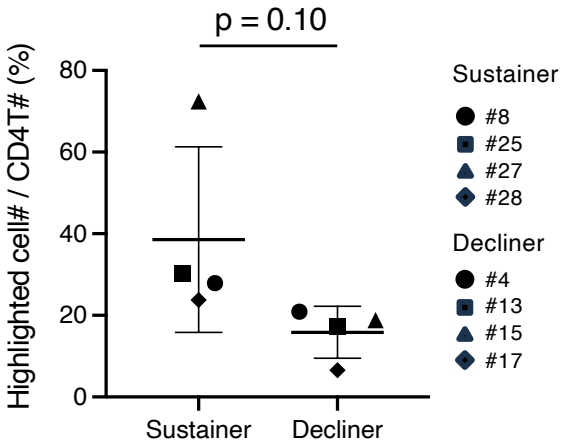

Fig. S3. Sustainer individuals had more cells in the circled region than decliner individuals.

(**A**) UMAP projection of single-cell analysis of post-vaccinated samples shown in individuals. (**B**) The percentage of circled cells in (A) in CD4+ T cells of each individual is shown. *P* value was calculated using t-test.

Fig. S4

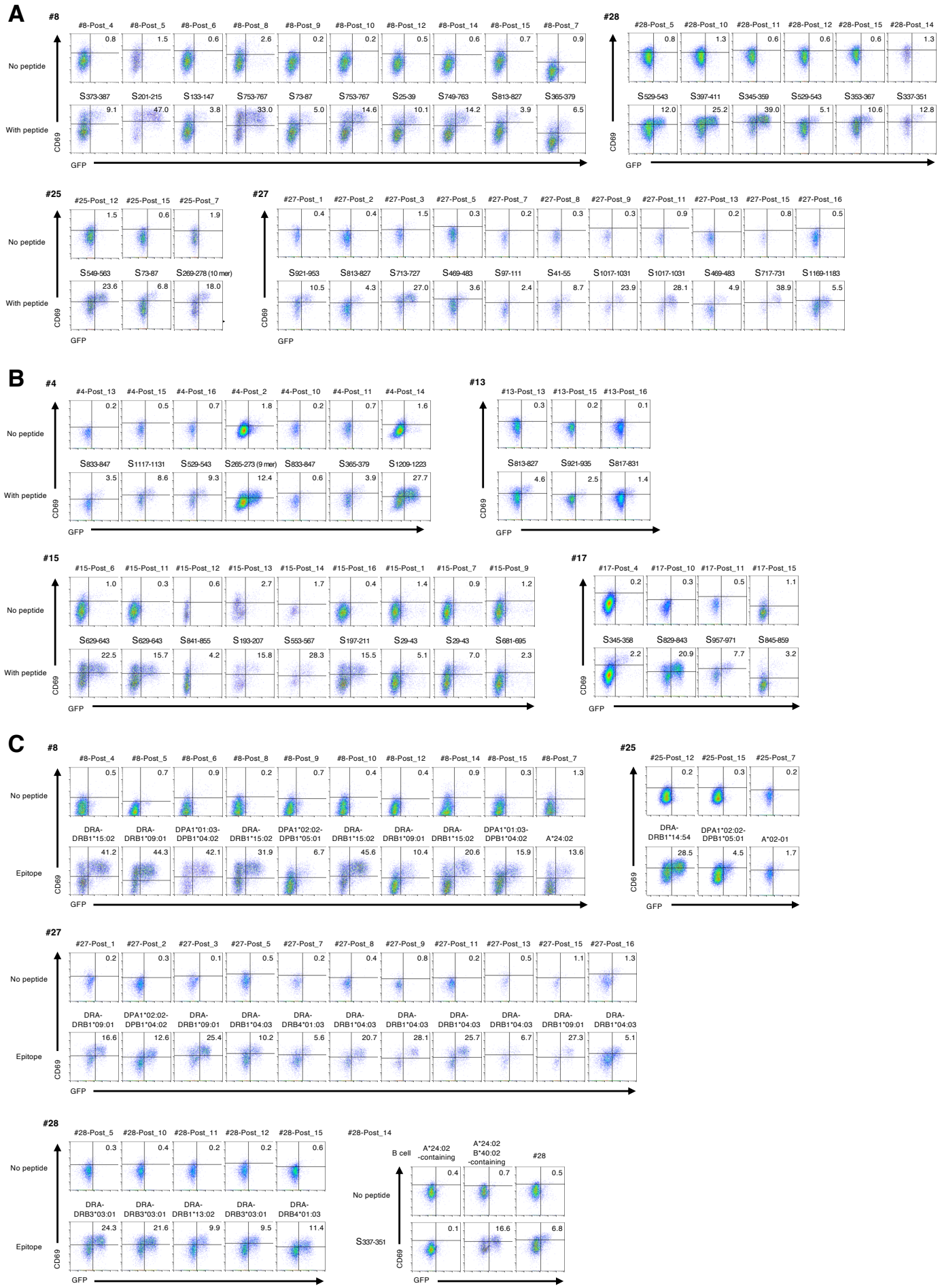
A
#8
#8-Post_4 #8-Post_5 #8-Post_6 #8-Post_8 #8-Post_9 #8-Post_10 #8-Post_12 #8-Post_14 #8-Post_15 #8-Post_7
0.8 1.5 0.6 2.6 0.2 0.2 0.5 0.6 0.7 0.9
S373-387 S201-215 S133-147 S753-767 S73-87 S753-767 S25-39 S749-763 S813-827 S365-379
9.1 47.0 3.8 33.0 5.0 14.6 10.1 14.2 3.9 6.5
#28
#28-Post_5 #28-Post_10 #28-Post_11 #28-Post_12 #28-Post_15 #28-Post_14
0.8 1.3 0.6 0.6 0.6 1.3
S529-543 S397-411 S345-359 S529-543 S353-367 S337-351
12.0 25.2 39.0 5.1 10.6 12.8
#25
#25-Post_12 #25-Post_15 #25-Post_7
1.5 0.6 1.9
S549-563 S73-87 S269-278 (10 mer)
23.6 6.8 18.0
#27
#27-Post_1 #27-Post_2 #27-Post_3 #27-Post_5 #27-Post_7 #27-Post_8 #27-Post_9 #27-Post_11 #27-Post_13 #27-Post_15 #27-Post_16
0.4 0.4 1.5 0.3 0.2 0.3 0.3 0.9 0.2 0.8 0.5
S921-953 S813-827 S713-727 S469-483 S97-111 S41-55 S1017-1031 S1017-1031 S469-483 S717-731 S1169-1183
10.5 4.3 27.0 3.6 2.4 8.7 23.9 28.1 4.9 38.9 5.5
No peptide
With peptide
CD69
GFP
B
#4
#4-Post_13 #4-Post_15 #4-Post_16 #4-Post_2 #4-Post_10 #4-Post_11 #4-Post_14
0.2 0.5 0.7 1.8 0.2 0.7 1.6
S833-847 S1117-1131 S529-543 S265-273 (9 mer) S833-847 S365-379 S1209-1223
3.5 8.6 9.3 12.4 0.6 3.9 27.7
#13
#13-Post_13 #13-Post_15 #13-Post_16
0.3 0.2 0.1
S813-827 S921-935 S817-831
4.6 2.5 1.4
#15
#15-Post_6 #15-Post_11 #15-Post_12 #15-Post_13 #15-Post_14 #15-Post_16 #15-Post_1 #15-Post_7 #15-Post_9
1.0 0.3 0.6 2.7 1.7 0.4 1.4 0.9 1.2
S629-643 S629-643 S841-855 S193-207 S553-567 S197-211 S29-43 S29-43 S681-695
22.5 15.7 4.2 15.8 28.3 15.5 5.1 7.0 2.3
#17
#17-Post_4 #17-Post_10 #17-Post_11 #17-Post_15
0.2 0.3 0.5 1.1
S345-358 S829-843 S957-971 S845-859
2.2 20.9 7.7 3.2
C
#8
#8-Post_4 #8-Post_5 #8-Post_6 #8-Post_8 #8-Post_9 #8-Post_10 #8-Post_12 #8-Post_14 #8-Post_15 #8-Post_7
0.5 0.7 0.9 0.2 0.7 0.4 0.4 0.9 0.3 1.3
DRA-DRB1*15:02 DRA-DRB1*09:01 DPA1*01:03-DPB1*04:02 DRA-DRB1*15:02 DPA1*02:02-DPB1*05:01 DRA-DRB1*15:02 DRA-DRB1*09:01 DRA-DRB1*15:02 DPA1*01:03-DPB1*04:02 A*24:02
41.2 44.3 42.1 31.9 6.7 45.6 10.4 20.6 15.9 13.6
#25
#25-Post_12 #25-Post_15 #25-Post_7
0.2 0.3 0.2
DRA-DRB1*14:54 DPA1*02:02-DPB1*05:01 A*02-01
28.5 4.5 1.7
#27
#27-Post_1 #27-Post_2 #27-Post_3 #27-Post_5 #27-Post_7 #27-Post_8 #27-Post_9 #27-Post_11 #27-Post_13 #27-Post_15 #27-Post_16
0.2 0.3 0.1 0.5 0.2 0.4 0.8 0.2 0.5 1.1 1.3
DRA-DRB1*09:01 DPA1*02:02-DPB1*04:02 DRA-DRB1*09:01 DRA-DRB1*04:03 DRA-DRB4*01:03 DRA-DRB1*04:03 DRA-DRB1*04:03 DRA-DRB1*04:03 DRA-DRB1*04:03 DRA-DRB1*09:01 DRA-DRB1*04:03
16.6 12.6 25.4 10.2 5.6 20.7 28.1 25.7 6.7 27.3 5.1
#28
#28-Post_5 #28-Post_10 #28-Post_11 #28-Post_12 #28-Post_15
0.3 0.4 0.2 0.2 0.6
DRA-DRB3*03:01 DRA-DRB3*03:01 DRA-DRB1*13:02 DRA-DRB3*03:01 DRA-DRB4*01:03
24.3 21.6 9.9 9.5 11.4
#28-Post_14
B cell
A*24:02 -containing
A*24:02 B*40:02 -containing
#28
0.4 0.7 0.5
S337-351
0.1 16.6 6.8
No peptide
Epitope
CD69
GFP

Fig. S4 continued

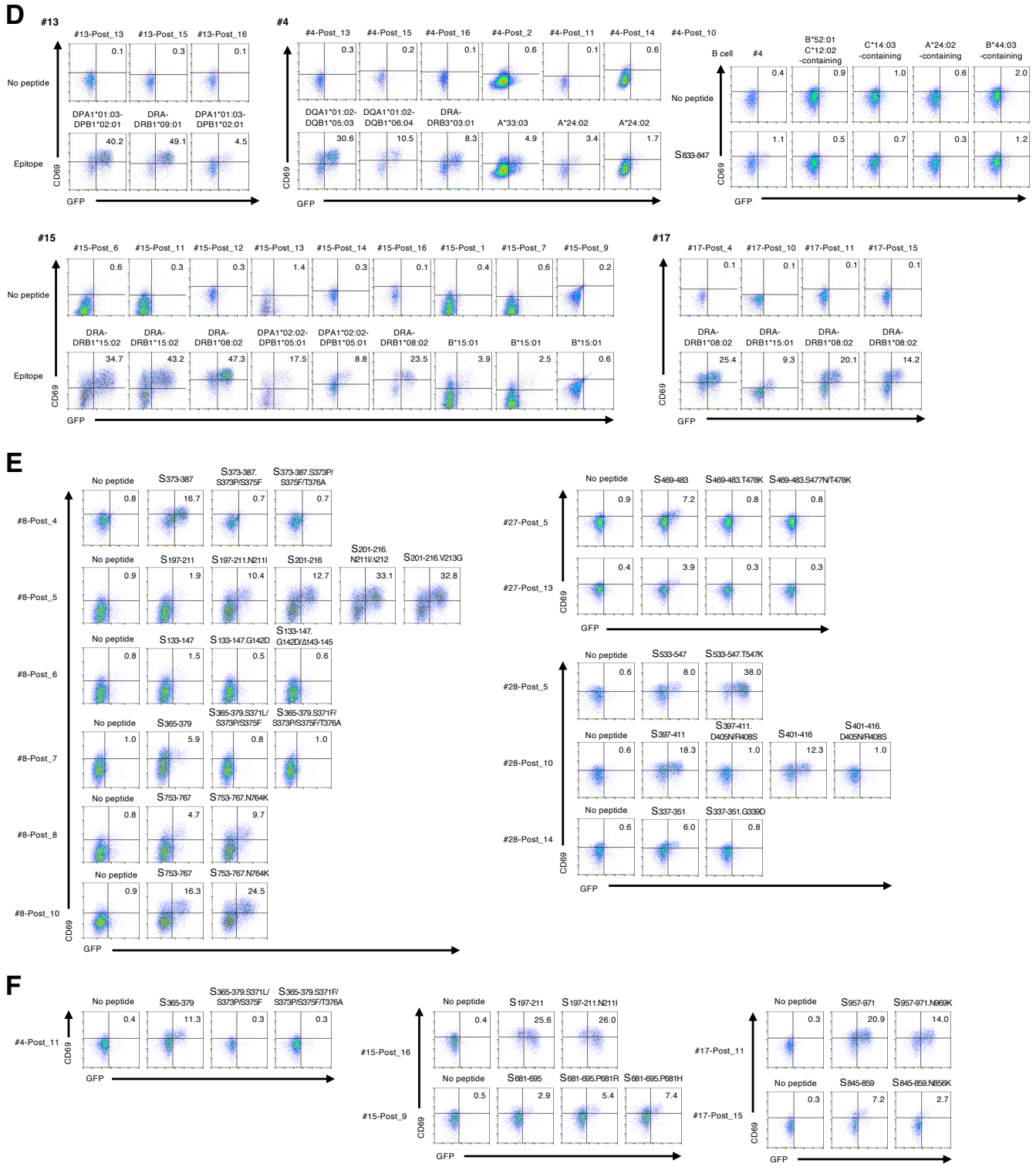

Fig. S4. Determination of S epitopes, restricting HLAs and mutated epitope antigenicity for post-vaccinated TCR clonotypes expanded in sustainers and decliners.

Reporter cells expressing TCRs were stimulated with 1 μg/ml of each S protein peptide in the presence of transformed B cells or HEK 293 T cells expressing indicated HLAs for overnight, and analyzed for GFP and CD69 expression. (**A** and **B**) Determination of S epitopes of TCR clonotypes expanded in sustainers (A) and decliners (B). (**C** and **D**) Determination of restricting HLAs of TCR clonotypes expanded in sustainers (C) and decliners (D). (**E** and **F**) Determination of antigenicity of mutated epitopes of TCR clonotypes expanded in sustainers (E) and decliners (F).

Fig. S5

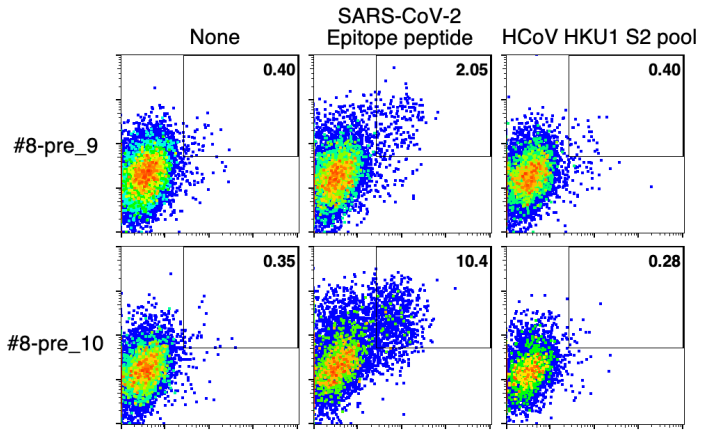

Fig. S5. The pre-existing S-reactive T cell clonotypes did not recognize HCoV epitopes. The only two clonotypes whose epitope sequences were relatively conserved in HCoV strains, donor #8-pre_9 and pre_10, were tested for their reactivity to the similar HCoV epitope counterparts. Reporter cell lines of these clonotypes were co-cultured with indicated antigens as well as APCs, and analyzed for GFP and CD69 expression.